J. Physiol. (1987), **387**, *pp.* 125–161
With 14 *text-figures*
Printed in Great Britain

NEUROTRANSMITTER-INDUCED CURRENTS IN RETINAL BIPOLAR CELLS OF THE AXOLOTL, *AMBYSTOMA MEXICANUM*

BY DAVID ATTWELL, PETER MOBBS, MARC TESSIER-LAVIGNE AND MARTIN WILSON*†

*From the Department of Physiology, University College London, Gower Street, London WC1E 6BT and the *Department of Zoology, University of California, Davis, CA 95616, U.S.A.*

(*Received 15 May 1986*)

SUMMARY

1. Whole-cell patch clamping was used to study the membrane properties of isolated bipolar cells and the currents evoked in them by putative retinal neurotransmitters.

2. Isolated bipolar cells show an approximately ohmic response to voltage steps over most of the physiological response range, with an average input resistance of 1·3 GΩ and resting potential of −35 mV. These values are underestimates because of the shunting effect of the seal between the patch electrode and the cell membrane. Depolarization beyond −30 mV produces rapid activation (10–100 ms) of an outward current (carried largely by potassium ions), which then inactivates slowly (0·5–2 s).

3. Of five candidates for the photoreceptor transmitter, four (aspartate, *N*-acetylhistidine, cadaverine, putrescine) had no effect on bipolar cells. The fifth substance, L-glutamate, opened ionic channels with a mean reversal potential of −12 mV in some cells (presumed hyperpolarizing bipolar cells), and closed channels with a mean reversal potential of −13 mV in other cells (presumed depolarizing bipolar cells).

4. The conductance increase induced by glutamate in presumed hyperpolarizing bipolar cells was associated with an increase in membrane current noise. Noise analysis suggested a single-channel conductance for the glutamate-gated channel of 5·4 pS. The power spectrum of the noise increase required the sum of two Lorentzian curves to fit it, suggesting that the channel can exist in three states.

5. The conductance decrease induced by glutamate in presumed depolarizing bipolar cells was associated with a decrease in membrane current noise that could be described as the sum of two Lorentzian spectra, and which suggested a single-channel conductance of 11 pS. The noise decrease implies that the channels closed by glutamate are not all open in the absence of the transmitter.

6. GABA (γ-aminobutyric acid) and glycine, transmitters believed to mediate lateral inhibition in the retina, open chloride channels in isolated bipolar cells, and increase the membrane current noise. Noise analysis suggested that the channels gated by GABA and glycine have conductances of 4·4 and 7·5 pS respectively. The noise spectra required the sum of two Lorentzian curves to fit them.

† To whom all reprint requests should be sent.

7. By whole-cell patch clamping cells in retinal slices, the synaptic transmitter released by photoreceptors was shown to close channels with an extrapolated reversal potential around −3 mV in depolarizing bipolar cells. The membrane properties of depolarizing bipolar cells in the retina were similar to those of isolated bipolar cells, except that their membrane capacitance was twice as large and their input resistance was one-tenth as large as for isolated cells.

8. We conclude that the time-dependent potassium current in axolotl bipolar cells plays little role in shaping the bipolar cells' light response because it is not significantly activated in the physiological potential range. The conductances modulated by the putative photoreceptor and lateral inhibitory transmitters are comparable to the cell conductance in the absence of transmitter. The voltage noise produced by the ionic channels in the bipolar cell membrane may hinder the detection of dim stimuli by these cells.

INTRODUCTION

Several aspects of retinal bipolar cells' function make an understanding of their membrane currents important. First, the photoreceptor–bipolar synapse is the first place in the visual system where information is separated into channels coding increases and decreases of illumination. Photoreceptors send output synapses to two classes of bipolar cell defined by their voltage response to light in the centre of their receptive field: 'depolarizing bipolar cells' which send output to 'on' ganglion cells, and 'hyperpolarizing bipolar cells' which project to 'off' ganglion cells (Miller & Dacheux, 1976). Secondly, lateral input to bipolar cells via horizontal cells produces an antagonistic surround to the bipolar cell receptive field (Werblin & Dowling, 1969). This centre–surround organization is passed on to retinal ganglion cells, and is believed to be important in contrast enhancement, in edge detection, and in removing redundancy in the visual information leaving the retina (Schantz & Naka, 1976; Marr & Hildreth, 1980; Srinivasan, Laughlin & Dubs, 1982). Thirdly, the voltage response of bipolar cells to light is more transient than that of the photoreceptors (Schwartz, 1974; Ashmore & Falk, 1980; Ashmore & Copenhagen, 1980), possibly due to shaping during synaptic transmission or by voltage-gated currents in the bipolar cell membrane. Transience in the response of cells with centre–surround receptive fields has been suggested to be important in motion detection (Marr & Ullman, 1981). Lastly, detection of dim stimuli by the retina requires that the voltage produced by these stimuli in bipolar cells is greater than any voltage noise produced by the random opening and closing of ion channels in the bipolar cell membrane (Falk & Fatt, 1974).

We have studied the membrane currents in bipolar cells isolated from the enzymatically dissociated retina, and in bipolar cells in retinal slices. The isolated cell preparation allowed us to characterize the response of the cells to putative retinal neurotransmitters without the complications of interpretation arising from the wealth of synaptic connexions, and the existence of neurotransmitter uptake mechanisms in the intact retina. The neurotransmitters tested were glutamate, aspartate, cadaverine, putrescine and *N*-acetylhistidine, which are known to be released from photoreceptors on depolarization and have been suggested as candidates for the photoreceptor transmitter (Cervetto & MacNichol, 1972; Murakami,

Ohtsu & Ohtsuka, 1972; Shiells, Falk & Naghshineh, 1981; Slaughter & Miller, 1981, 1983*a*, 1985; Miller & Schwartz, 1983), and γ-aminobutyric acid (GABA) and glycine, which are thought to mediate inhibitory input to bipolar cells from horizontal, amacrine and interplexiform cells (Hollyfield, Rayborn, Sarthy & Lam, 1979; Chiu & Lam, 1980; Rayborn, Sarthy, Lam & Hollyfield, 1981; Miller, Frumkes, Slaughter & Dacheux, 1981; Wu, 1986). Use of the retinal slice preparation allowed a comparison of the properties of isolated cells with those of cells in the retina. Cells were voltage clamped using the whole-cell variant of the patch-clamp technique (Hamill, Marty, Neher, Sakmann & Sigworth, 1981).

METHODS

Experiments were carried out on retinae removed from recently killed axolotls (*Ambystoma mexicanum*), 12–20 cm long.

Isolated cells

Isolated bipolar cells were obtained using the method of Bader, MacLeish & Schwartz (1979). Briefly, an isolated retina was incubated in 2 ml of a stirred solution containing (mM): NaCl, 66; KCl, 3·7; $NaHCO_3$, 25; NaH_2PO_4, 10; sodium pyruvate, 1; DL-cysteine HCl (Sigma), 10; and 0·02 ml papain (Sigma P3125 or Cooper Biomedical 3126), pH 6·9, bubbled with 95 % O_2–5 % CO_2. The retina was then rinsed three times in 15 ml of a solution containing (mM): NaCl, 96; KCl, 3·7; NaH_2PO_4, 0·25; KH_2PO_4, 0·4; sodium pyruvate, 1; glucose, 1; HEPES, 2; pH 7·25, and then gently triturated approximately 20–30 times in a Pasteur pipette before plating into the recording chamber. This procedure was carried out in normal room lighting. Cells were used up to 3 h after retinal dissociation; after this period they tended to retract their processes and become unrecognizable.

Bipolar cells were identified by their characteristic morphology (see Fig. 1), with a Landolt club (Landolt, 1871; Cajal, 1893) at one end of the soma, and an axon at the other end. All the cells in the *Ambystoma* retina have Landolt clubs (Lasansky, 1973). Dendrites were often seen at the Landolt club end of the cell, but these (and the axon) were often much shorter (typically 10–30 μm) than is seen for dye-filled bipolar cells in the intact retina, presumably because of damage in the isolation procedure. Because of this shortening of the cells' processes, it was not possible to distinguish depolarizing and hyperpolarizing bipolars on the basis of their axon lengths. (In the intact retina the axons of the depolarizing bipolars terminate in the proximal part of the inner plexiform layer, and thus are longer than those of the hyperpolarizing bipolars which end in the distal part of the inner plexiform layer. In *Ambystoma* this is the only shape difference between depolarizing and hyperpolarizing bipolars: Lasansky, 1978.) Nevertheless, the responses of isolated bipolar cells to glutamate, presented in this paper, suggest both depolarizing and hyperpolarizing cells survive the isolation procedure.

The results reported in this paper were obtained by patch clamping over 500 isolated bipolar cells. Unless otherwise stated, each result was obtained in at least six different cells.

Cells in retinal slices

Retinal slices were used to study the properties of bipolar cells in the retina, because this preparation allows patch recording electrodes to be moved up to a cell's membrane surface for giga-seal formation.

Retinal slices, 100–200 μm thick, were obtained by cutting an isolated flat-mounted retina with a razor blade, as described by Werblin (1978). Slices were mounted transversely so that all the retinal cell types were visible. Apart from removal of the eyes from the animal (done under dim red light) all manipulations were performed using infra-red illumination and an image converter, in order to preserve the cells' light responses.

Bipolar cells were initially identified by their appearance in the slice, with a cell body near the outer plexiform layer, and an axon descending towards the inner plexiform layer. This identification was confirmed by the cell's light response and sometimes by subsequent observation of the cell's morphology using fluorescence microscopy: the fluorescent dye Lucifer Yellow was

included in the patch recording electrode (1 mg ml^{-1}) and entered the cell following rupture of the membrane patch when passing to whole-cell clamp mode. An example of a Lucifer-Yellow-filled cell is shown in Fig. 8.

Solutions

The superfusion solution outside the cells consisted of (mM): NaCl, 88; KCl, 1·5; $CaCl_2$, 3; $MgCl_2$, 0·5; $NaHCO_3$, 0·5; NaH_2PO_4, 1; sodium pyruvate, 1; glucose, 15; HEPES, 20; pH adjusted to 7·25 with NaOH. The various solutions used to fill the patch pipettes are given in Table 1. Included in Table 1 are the free calcium concentrations calculated for the patch pipette solutions from the equilibrium constant for calcium ion binding to EGTA (Smith & Martell, 1976, 0·1 M ionic strength): measurements with a calcium-sensitive electrode showed that solutions with no added calcium or EGTA contained 17·5 μM-calcium (present as an impurity in reagents used to make the solutions).

TABLE 1. Internal solutions. These contained 13·3 mM-HEPES, plus the following ingredients (mM)

Solution	A 100 Cl_i^-	B 30 Cl_i^-	C 30 Cl_i^- + ATP	D 10 Cl_i^-	E Low EGTA	F High EGTA
KCl	100	30	30	10	30	16·5
Potassium acetate	—	70	70	90	70	70
EGTA	0·6	0·6	0·6	0·6	0·02	5
$CaCl_2$	—	—	—	—	—	0·5
$MgCl_2$	—	—	2	—	—	—
ATP	—	—	1	—	—	—
NaCl	—	—	—	—	—	6
NaOH	5·4	4·4	6·0	4·4	3·0	—
KOH	—	—	—	—	—	16·2
Calculated free calcium concentration	11·3 nM	11·3 nM	11·9 nM	11·3 nM	1·5 μM	42 nM
Tip potential (mV)	−2·5	−5·8	−5·8	−7	−5	−5·8

The pH was adjusted to 7·0 with NaOH or KOH as listed. Solutions to which no calcium was added contained approximately 17·5 μM-calcium (an impurity in the reagents used to make the solutions).

During whole-cell clamping, small ions in the patch-pipette solution diffuse into the cell in 30–60 s (Fenwick, Marty & Neher, 1982). By using different pipette solutions from Table 1, we could study cells with different internal chloride concentrations and different internal calcium concentrations and buffering strengths.

Drug application

Neurotransmitter candidates were applied either by local superfusion or by ionophoresis using a constant current source from a micro-electrode. For local perfusion, the drugs were dissolved in normal external solution and pressure-ejected from a small pipette held near the cell. For ionophoresis, micro-electrodes filled with a concentrated solution of the drug under study (resistance 30 MΩ when in the external solution) were used. GABA and glycine were ionophoresed with positive current (1–10 nA) from 0·5 M solutions at pH 3. L-glutamate and L-aspartate were ionophoresed with negative current (1–10 nA) from a 1 M-sodium salt solution at pH 8 and a 200 mM-sodium salt solution at pH 8·5, respectively. Bicuculline and strychnine were ejected with positive current (10–40 nA) from 10 mM solutions at pH 4 and pH 5·5 respectively. Backing currents of 1–10 nA were used to minimize loss of drug from the electrode when no ejection current was applied. Ionophoresis and local superfusion of drugs gave similar results.

Patch electrodes, series resistance and tip potentials

Recordings were made using a List EPC-5 or EPC-7 patch clamp. Capacity currents were subtracted electronically (Hamill *et al.* 1981). Electrodes were pulled on a BBCH puller (Mecanex, Geneva) from Clark Electromedical GC150TF glass, and had resistances in the range 3–10 MΩ before forming a seal. Cell-attached seal resistances of over 20 GΩ were sometimes obtained, but usual values were in the range 1–10 GΩ.

After obtaining a cell-attached seal on a bipolar cell, the membrane patch under the patch pipette was ruptured by gentle suction applied to the rear of the pipette, to obtain a whole-cell voltage clamp. The elctrode resistance was then typically 10–30 MΩ (measured from the current response to a voltage-clamp step), although values as low as 4 MΩ and as high as 60 MΩ were sometimes found. This series resistance often increased during the course of an experiment, and thus had to be frequently monitored. The voltage error (series resistance × current flowing) produced by the series resistance was corrected for by subtraction from the nominal voltage-clamp potential. When the current varied with time during a voltage-clamp pulse, the *average* value of current was used in this calculation; however, when the product of the series resistance and the change in current during a pulse was greater than 5 mV, the data were discarded.

Tip potentials were corrected for as described by Fenwick *et al.* (1982). The tip potentials measured in normal external solution for the different internal solutions used are given in Table 1. These tip potentials were added to the apparent membrane potential.

Voltage-clamp quality

On applying a command voltage change ΔV to the patch clamp, the charging of the membrane capacitance, C, is limited by the series resistance, R_p, at the mouth of the patch pipette. If the cell membrane resistance is R_m, the time constant with which the membrane potential approaches its steady-state value, $R_m \Delta V/(R_m + R_p)$, is $\tau = CR_m R_p/(R_m + R_p)$. This time constant was in the range 0·05–0·5 ms.

The non-spherical shape of bipolar cells (Fig.1) raises the question of how uniform the potential is in these cells when voltage clamping. Taking a typical input resistance (in the physiological potential range) for an isolated cell of 1·3 GΩ, and an apparent membrane area of 793 μm^2 (measured from video recordings with a TV camera attached to the microscope), we can calculate a membrane conductance per unit area of 0·97 S m^{-2} (assuming the conductance to be uniformly distributed). For dendrites or axons about 1 μm in diameter, as in Fig. 1, filled with cytoplasm of resistivity 2 Ω m, this would lead to a d.c. electrical space constant of 360 μm, i.e. much longer than the length of the dendrites or axons of isolated cells (typically 20 μm). At depolarized potentials, where the slope resistance is about ten times lower (see Fig. 2) this space constant would become 114 μm.

The space constant for high-frequency current fluctuations will be shorter than these d.c. values, because of current flow through the membrane capacitance. If the specific membrane capacitance is 1 $\mu F\ cm^{-2}$, then a 1 μm diameter process with properties as described above would, in the physiological potential range, have a space constant of 63 μm at a frequency of 500 Hz (typically the highest frequency of relevance in our noise analysis). At depolarized potentials, the 500 Hz space constant would be 62 μm. The dendrites and axons on our isolated cells typically have lengths of 20 μm. Even taking the lowest value calculated for the a.c. space constant (62 μm), if the cell processes have sealed ends it is possible to calculate that the fractional voltage non-uniformity along a 20 μm process will be only 5%.

Thus, unless there is substantial non-uniformity of membrane conductance, with most of the conductance concentrated in the dendrites and axons, the voltage-clamped cell should be essentially uniform in potential.

Noise analysis

Samples of data, 5–200 s long, were digitized off-line, and divided into 0·25–2 s subsamples, after low-pass filtering (8-pole, Butterworth) at less than half the sampling frequency and high-pass filtering at a frequency greater than the reciprocal of the subsample length. A PDP-11/73 computer was used to calculate the variance and power spectra of the data. Power spectra were taken as the average of the fast Fourier transform (Bendat & Piersol, 1971) of at least five subsamples of membrane current. Instrumentation noise, measured with the patch pipette removed from the

solution or with the pipette in the solution with its tip sealed (and thus of infinite resistance), was negligible. Data were discarded if filtering by the pipette series resistance (half-power frequency $1/(2\pi CR_p)$, typically 500–2000 Hz) was significant in the frequency range of interest.

Power spectrum fitting

Power spectra obtained from noise analysis were fitted with theoretical curves (sums of Lorentzian spectra) using the methods of Colquhoun, Dreher & Sheridan (1979).

The spectra we obtained (Figs. 5, 6 and 14) required the sum of two Lorentzian spectra to fit them (consistent with the channels studied having three or more kinetically distinguishable states: see pp. 139 and 145). Representing the spectra as the sum of more than two Lorentzian spectra (as would be required if there were more than three distinct states), might slightly improve the fit of the theoretical curves to the data, because of the increased number of parameters which can be adjusted to obtain a fit. However, we feel that the accuracy of our spectral data, and the restricted frequency range over which we can study the noise (with an upper limit of about 800 Hz in our best cells due to filtering by the series resistance of the patch pipette), do not warrant representation of the spectra by the sum of more than two Lorentzian curves.

We considered the possibility that our spectra required more than one Lorentzian curve to fit them because the concentration of transmitter ejected from the ionophoretic or perfusion pipette was not uniform all over the cell, and that if the drug concentration were uniform the spectrum would be a single Lorentzian. The following analysis rules out that possibility. For a two-state channel model, with a single Lorentzian spectrum, if the transmitter concentration is low enough for the channel opening probability to be low (as the linear plots of noise variance against mean current in Figs. 5 and 14*B* show), the half-power frequency of the Lorentzian spectrum is independent of the transmitter concentration (Colquhoun & Hawkes, 1977). Thus, although the transmitter concentration may be lower at points on the cell further from the source of transmitter so that less current (and less associated noise) are generated at that part of the cell, the shape of the noise spectrum will be the same as that generated where the transmitter concentration is higher. The total noise spectrum for the whole cell will still be one Lorentzian.

Calculation of the single-channel conductance

The current flowing through a single channel was obtained as the ratio of the drug-induced noise variance to the drug-induced mean current, when the probability of channel opening was low (Colquhoun & Hawkes, 1977), and was divided by the difference between the clamping potential and the reversal potential to obtain the single-channel conductance. Since data were filtered prior to carrying out noise analysis (for example, high-pass filtered at 2 Hz and low-pass filtered at 500 Hz) some of the drug-induced noise variance will be filtered out. This was corrected for by using the sum of the Lorentzian curves fitted to the spectra. Extrapolating these to zero and infinite frequency, we could calculate the fraction of the variance lost by filtering. This fraction was typically 10%.

RESULTS

Membrane properties of isolated bipolar cells

Examples of isolated bipolar cells are shown in Fig. 1. Ionic currents, evoked in an isolated bipolar cell by voltage-clamp steps from a holding potential of −58 mV are shown in Fig. 2. Over most of the physiological response range of bipolar cells the ionic current was time independent and roughly ohmic, with a mean input resistance at −50 mV of $1{\cdot}3 \pm 2{\cdot}2$ GΩ (mean ± S.D., $n = 106$ cells studied with 30 mM-chloride solution in the patch pipette, i.e. solution B or C from Table 1). The average value of capacitance, derived from the capacity current flowing at the onset of a voltage-clamp step, was $11{\cdot}4 \pm 4{\cdot}5$ pF ($n = 174$ cells). The mean resting potential of the cells, defined as the potential for which no pipette current flows in whole-cell clamp mode, was -35 ± 12 mV ($n = 62$ cells studied with solution B or C in the pipette). These values of resistance and resting potential must underestimate the true

values for the cells because of shunting by the seal between the cell membrane and the patch pipette, the resistance of which (measured as 1–10 GΩ when cell-attached before going to whole-cell recording mode) was not infinitely greater than the measured input resistance in whole-cell mode. No evidence was found for cells' resting

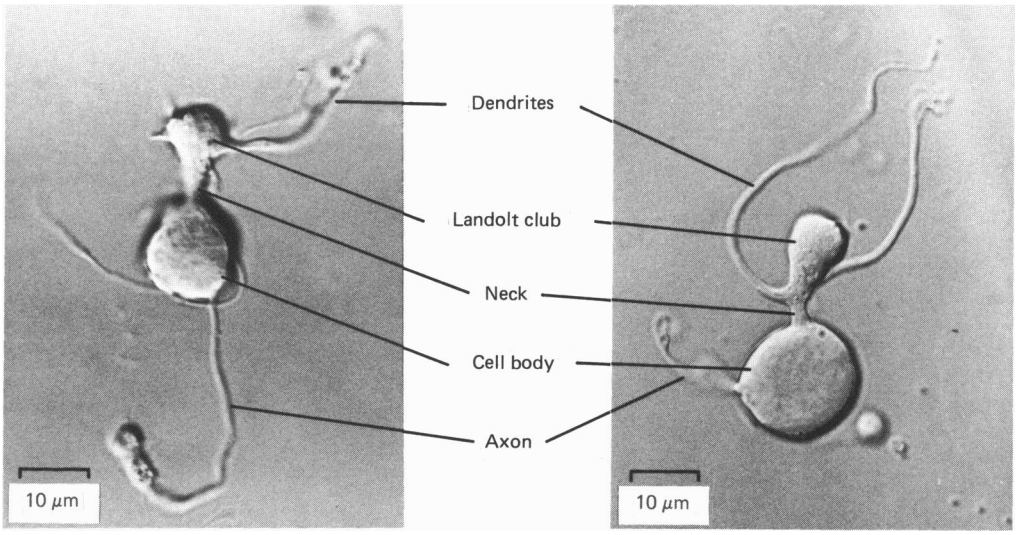

Fig. 1. Two bipolar cells, isolated by the methods described in the text, viewed with Nomarski optics. The Landolt club, a characteristic process found only on bipolar cells, which we used to identify the cells, is clearly visible.

potentials falling into two classes, which might represent depolarizing and hyperpolarizing cells. Nevertheless, the two classes of response to glutamate described below suggest that both types of bipolar cell survive the isolation procedure.

Depolarization beyond −30 mV evoked a rapid time-dependent increase of outward current, which then decayed more slowly (Fig. 2). The wave form of this time-dependent current could be inverted when cells were bathed in solution with all the sodium replaced by potassium (i.e. depolarizing to potentials above −30 mV but below the Nernst potential for potassium ions evoked, after an instantaneous jump, a rapid decrease of outward current followed by a slow increase of outward current). Furthermore, filling the patch pipette with solutions in which all the potassium was replaced by choline or caesium abolished the outward current. It appears, therefore, that a time-dependent potassium conductance, qualitatively similar to that seen in molluscan neurones and T lymphocytes (Connor & Stevens, 1971*a*, *b*; Fukushima, Hagiwara & Henkart, 1984; Cahalan, Chandy, DeCoursey & Gupta, 1985), generates the changes of current seen in Fig. 2 for depolarization above −30 mV. Applying hyperpolarizing pre-pulses increased the amplitude of the time-dependent current evoked on depolarization, possibly due to a removal of inactivation of the current (Cahalan *et al.* 1985), but did not move its voltage range of activation more into the physiological response range of bipolar cells. A full analysis of this current will be published elsewhere. The time-dependent current was seen in 90 % of isolated bipolar cells. In the remaining 10 % of cells the membrane

current–voltage relation was time independent, although showing some outward rectification above −30 mV.

The membrane currents in Fig. 2 were obtained with pipettes containing 30 mM-chloride ions and $1{\cdot}1 \times 10^{-8}$M-calcium ions (solution C from Table 1). Membrane

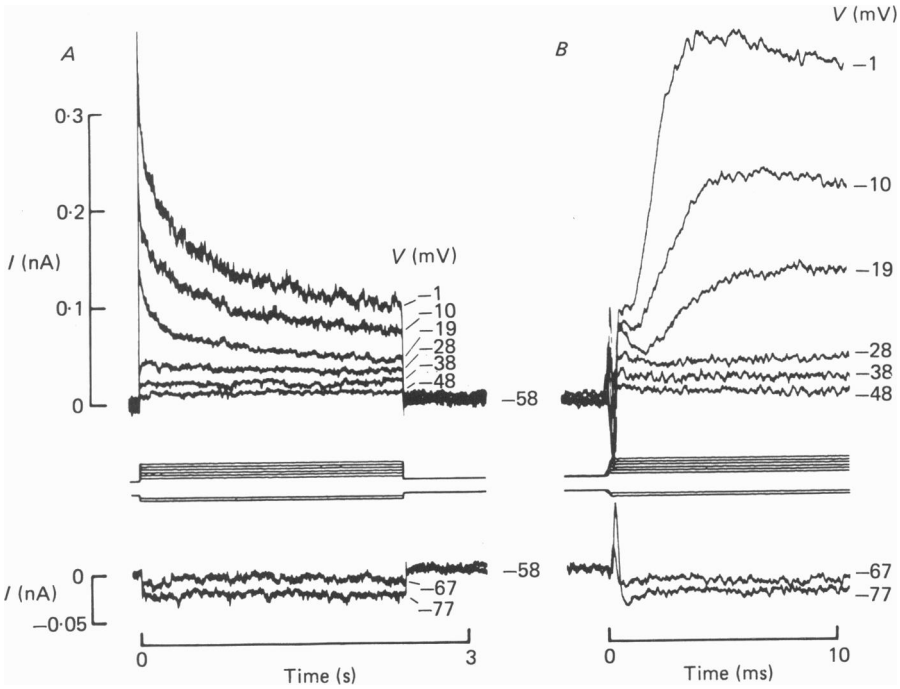

Fig. 2. Ionic currents in the membrane of an isolated bipolar cell (solution C of Table 1 in the patch pipette). The cell was voltage clamped to different potentials (shown by each trace) from a holding potential of −58 mV. Responses are shown on a slow time base in *A*, with onsets on a fast time base in *B*. The biphasic current change seen in *B* as a fast transient in the first 0·5 ms after changing the voltage, and as a slower sag in the current extending to 1·5 ms (particularly clear in the records for −77 and −19 mV), is due to imperfect electronic subtraction of the current charging the capacitance of the cell and pipette. Depolarization past −30 mV produces a rapid increase (*B*) followed by a slow decrease (*A*) in outward current. The slope resistance of this cell was 1 GΩ near −60 mV, and 70 MΩ near 0 mV for the peak current–voltage relation. The seal resistance when cell-attached, before going to whole-cell mode, was 4 GΩ. The pipette series resistance was 16 MΩ.

currents were not significantly different when ATP was included in (solution C) or omitted from (solution B) the pipette, when internal chloride was altered to 10 or 100 mM (solutions A or D), when the calcium concentration was raised to 1·5 μM (solution E), or when the calcium buffering power of the pipette solution was raised by including 5 mM-EGTA (solution F).

The contribution of non-synaptic current noise to bipolar cell voltage noise

Detection of dim stimuli by bipolar cells requires that these stimuli evoke a voltage change larger than the voltage noise generated in the dark by ion channels in the

cell membrane. To evaluate the voltage noise produced by channels which are not gated by neurotransmitters, we measured the power spectrum of the current noise when cells were voltage clamped at −50 mV, i.e. near their physiological dark potential. (The voltage dependence of the noise will be published elsewhere.) In seven cells identified from their response to glutamate (described below) as hyperpolarizing bipolar cells, the current variance (in the range 0–400 Hz) was $1{\cdot}19 \pm 0{\cdot}56$ pA^2, while in seven cells identified as depolarizing bipolar cells the corresponding figure was $41{\cdot}7 \pm 39{\cdot}7$ pA^2. The larger noise in isolated depolarizing cells is caused by the presence of open glutamate-sensitive channels (see Fig. 7).

To calculate the contribution of non-synaptic channels to membrane voltage noise we took the spectrum of current fluctuations obtained for isolated hyperpolarizing cells and, to mimic filtering by the membrane capacitance in the conversion of current to voltage, divided the current variance at each frequency f by a factor: $1 + (2\pi\tau_m f)^2$, where the membrane time constant, τ_m, was set to 2·7 ms, as found for bipolar cells in retinal slices (see below). The standard deviation of the filtered fluctuations was then obtained as the square root of the area under the filtered spectrum and converted to the standard deviation of the resulting voltage fluctuations by multiplying by the mean input resistance of 120 MΩ found for cells in retinal slices (see below). The result was 106 ± 30 μV ($n = 7$).

An assumption implicit in this calculation is that the lower resistance of bipolars in retinal slices, as compared with isolated cells, is due to synaptic conductance not present in isolated cells, whose noise contribution is not considered in this calculation. If the higher input resistance for isolated cells reflects, however, merely a loss of cell processes or electrical coupling during the isolation procedure (see Discussion), and the missing membrane contributes current noise with the same properties as that found in isolated cells, then an upper limit to the voltage noise produced in a cell in the intact retina can be estimated by multiplying the figure of 106 μV calculated above by the square root of the ratio of input resistances of isolated and slice bipolar cells, i.e. a factor of 3, giving voltage noise with a standard deviation of 318 μV.

Candidates for the photoreceptor transmitter

Of the five substances found to be synthesized by, and released from photoreceptors on depolarization, which are candidates for the photoreceptor transmitter (Miller & Schwartz, 1983), only glutamate induced current changes in our isolated bipolar cells. L-Aspartate (perfused at 100 μm on three cells, 200 μm on eight cells, 500 μm on sixteen cells, and ionophoresed onto five cells), *N*-acetylhistidine (perfused at 200 μM on twelve cells and 500 μm on sixteen cells), cadaverine (500 μm on twenty cells) and putrescine (500 μm on twenty cells) had no effect. Aspartate had no effect at positive membrane potentials, ruling out the possibility that the lack of effect in the physiological potential range was due to magnesium block of *N*-methyl D-aspartate receptors (Nowak, Bregestovski, Ascher, Herbert & Prochiantz, 1984). These results suggest that glutamate is the photoreceptor transmitter, consistent with the results of Slaughter & Miller (1983*a*, *b*), Ishida, Kaneko & Tachibana (1984) and Lasater, Dowling & Ripps (1984).

The effects of glutamate on isolated bipolar cells could be divided into two classes. In 38 of the 227 cells (17%) to which glutamate was applied, glutamate evoked an

inward current in the physiological potential range. This response was associated with an increase in membrane conductance in all twenty-two cells for which this was tested (see below). In 36 of the 227 cells (16%), glutamate evoked an outward current in the physiological range. This response was associated with a decrease in membrane conductance in all twenty-four cells for which this was tested (see below). In the remaining 153 of the 227 cells (67%), glutamate had no effect. The number of cells responding to glutamate varied widely between preparations. Frequently, none of the bipolar cells obtained from a particular preparation responded to glutamate. In most preparations where responding cells were found, cells of both classes (inward current and outward current evoked by glutamate) were found, provided the glutamate concentration was high enough (see below). In some preparations, only cells of one class were found. The low yield of glutamate-responding cells is similar to the findings of Lasater *et al.* (1984) for isolated skate bipolar cells, and presumably occurs because the enzymatic isolation procedure either removes the cell processes where the glutamate receptors are located, or in some way degrades the receptors or the channels they control.

The glutamate-induced conductance increase

Fig. 3*A* shows the membrane current changes induced by ionophoretically applied glutamate in an isolated bipolar cell where glutamate increased the membrane conductance, presumably by opening channels in the cell membrane. Below 0 mV glutamate evoked an inward current, and above 0 mV an outward current was produced. The current–voltage relation for the glutamate-induced current (Fig. 3*B*) exhibits outward rectification about the reversal potential. Similar results were found when glutamate (100 μM–1 mM) was applied by local perfusion (see Methods) instead of by ionophoresis. We never observed a decrease in the amplitude of the glutamate-induced current at potentials below −60 mV, as seen by Tachibana (1985) for the effect of glutamate on isolated carp horizontal cells.

We made many attempts to determine where on the cell the glutamate receptors were located, by moving the ionophoretic pipette (or local perfusion pipette) to different parts of the cell, applying the drug and looking for a variation in the response size or time course. These attempts were unsuccessful, in that the response was not greatly affected by the pipette position, probably because the small size of the cells (see Fig. 1) made it difficult to apply drug to a very small fraction of the cell surface area, and because the dendrites and axon of the cell were rarely laid out in positions where glutamate could be applied to one of them without being applied to other parts of the cell. (Furthermore, Ishida *et al.* (1984) have found that glutamate sensitivity in isolated horizontal cells is relatively diffusely distributed, possibly because there are 'extrajunctional' receptors at parts of the cell which do not normally receive synaptic input or because junctional receptors are relocated to the soma when dendrites retract after cells are isolated.) We assume that the receptors being studied have the same properties as those which are normally activated by the transmitter released from photoreceptors. This is consistent with the fact that glutamate can induce either an inward current or an outward current in the physiological potential range, as would be expected for its acting on hyperpolarizing and depolarizing bipolar cells (see below).

Most of the cells to which we applied glutamate were studied with patch pipettes

containing 30 mM-Cl^- (solutions C or E from Table 1). The average reversal potential found for the conductance increase induced by glutamate was $-12{\cdot}2 \pm 13{\cdot}8$ mV ($n = 7$). There was no significant difference between the reversal potentials found when the calcium concentration inside the patch pipette (and hence inside the cell)

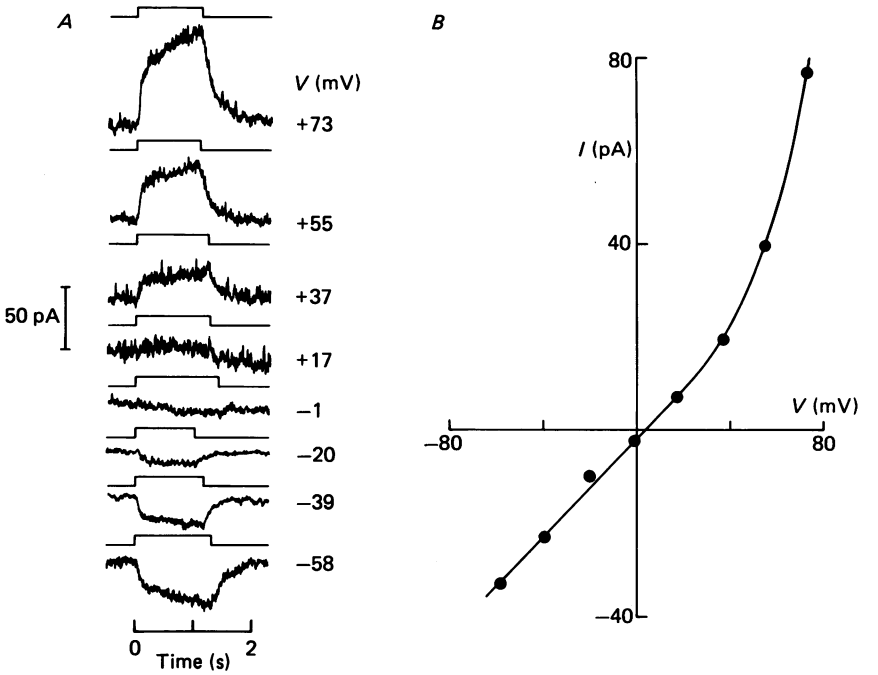

Fig. 3. *A*, currents induced by ionophoretic application of glutamate in an isolated bipolar cell, voltage clamped to different membrane potentials (given beside each trace). This cell is presumed to be a hyperpolarizing bipolar cell because glutamate induces an inward current in the physiological potential range. Timing of ionophoresis shown by square traces above each current record. Ionophoretic pipette current was switched from a backing current of +10 nA to an ejection current of −10 nA for the periods shown (the periods differ slightly since they were controlled manually, rather than by a timing circuit). Solution E in the patch pipette. The slow increase in glutamate-evoked current, after the initial rapid onset, was not generally seen and may reflect diffusion of glutamate to receptors on the cell distant from the ionophoretic electrode. *B*, current–voltage relation for the glutamate-induced current, measured 1 s after the start of drug application.

was 12 nM (three cells with solution C in the pipette) or 1·5 μM (four cells with solution E). We have not carried out a systematic analysis of the ionic selectivity of the conductance increased by glutamate because of the small number of responding cells. The reversal potential of −12 mV suggests that glutamate modulates a relatively non-specific conductance carrying perhaps half sodium and half potassium ions. The channels opened by glutamate in isolated horizontal cells are permeable to cations, with poor selectivity (Tachibana, 1985).

The conductance increase induced by glutamate was comparable to the resting conductance of the cell (Fig. 7*A*): the mean conductance induced by 1 mM-glutamate

in four cells was 0·72 nS, while the input conductance in the absence of glutamate was around 0·5–1 nS (data are given for 1 mM concentration to allow comparison with data from conductance-decrease cells described below). Thus, the glutamate-gated conductance can exert significant control over the cell's membrane potential.

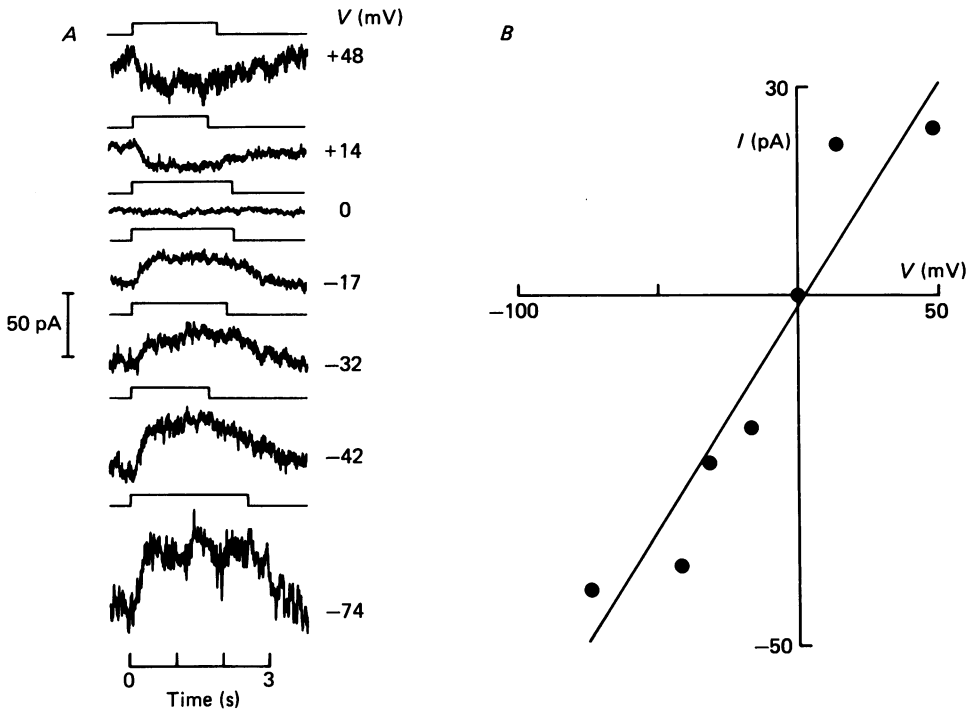

Fig. 4. *A*, current induced by 1 mM locally perfused glutamate in an isolated bipolar cell voltage clamped to different potentials (given beside each trace). This cell is believed to be a depolarizing bipolar because glutamate induces an outward current in the physiological potential range. Square traces above each response show the timing of applying pressure to eject glutamate-containing solution (the pressure pulse length was controlled manually, and so varies slightly from one run to another). *B*, current–voltage relation for the data in *A*, with outward current induced by glutamate shown as negative and inward current shown as positive. Solution B in the patch pipette.

The glutamate-induced conductance decrease

Fig. 4*A* shows data from a cell in which glutamate decreased the cell conductance, presumably by closing ionic channels in the cell membrane. In the physiological potential range glutamate induced an outward membrane current. Since neurotransmitter release is suppressed when photoreceptors are hyperpolarized by light, this class of cell would, in the retina, have an inward current induced in it by light, and we therefore postulate it to be a depolarizing bipolar cell. Conversely, the class of cells exemplified by Fig. 3, in which glutamate produces an inward current in the physiological range, are presumed to be hyperpolarizing bipolar cells.

The current–voltage relation in Fig. 4*B* for the current change evoked by glutamate is roughly ohmic, with a reversal potential near 0 mV. (Note that for this

current–voltage relation the outward current evoked by glutamate below 0 mV is plotted as negative, so the plot actually shows the current change evoked when glutamate is removed rather than applied.) For seven cells with solution containing 30 mM-Cl^- in the patch pipette (solution C from Table 1) the mean reversal potential was $-13{\cdot}3 \pm 8{\cdot}9$ mV, similar to the value found for the conductance increase produced by glutamate described above.

The magnitude of the conductance decrease induced by glutamate varied considerably between cells, and was loosely correlated with the conductance of the cell before applying glutamate (Fig. 7*A*). In six cells the mean conductance decrease induced by 1 mM-glutamate was 0·97 nS. The glutamate-modulated conductance can be a large fraction of the conductance of the cell in the absence of glutamate.

Cells in which glutamate evoked a conductance decrease were routinely found using 1 mM-glutamate, but only rarely found with lower concentrations or ionophoretic application of the drug (suggesting that ionophoretic application of glutamate usually resulted in a drug concentration at the cell of less than 1 mM). Glutamate-induced conductance increases, on the other hand, were routinely observed using ionophoretic application or local perfusion of 100 μM-glutamate. (Owing to the generally low proportion of responding cells, we did not test glutamate concentrations below 100 μM.) This suggests that depolarizing bipolar cells are less sensitive to the photoreceptor transmitter than hyperpolarizing bipolar cells are.

We also routinely observed that the kinetics of the response to glutamate were slower for those cells where glutamate produced a conductance decrease than for cells which gave a conductance increase. For five cells where 1 mM-glutamate decreased the conductance, and whose responses were stable enough to permit accurate measurement, the half-time for the onset of the response was $0{\cdot}94 \pm 0{\cdot}30$ s, while for four conductance-increase cells the corresponding figure was $0{\cdot}06 \pm 0{\cdot}04$ s. Half-times obtained with ionophoresis or with lower concentrations of glutamate were not significantly different from those obtained with perfusion of 1 mM-glutamate.

We considered the possibility that glutamate-induced conductance decreases occurred because applied glutamate was desensitizing an already present conductance *increase*, induced by a low background level of glutamate remaining in the bath from previous glutamate applications (cf. Ishida & Neyton, 1985). This seemed unlikely since experiments were performed in the presence of continuous perfusion of Ringer solution over the cells. It was ruled out by the observation of a glutamate-induced conductance decrease in the first cell studied in a preparation to which glutamate had never been applied previously.

Noise changes associated with the glutamate-induced conductance increase

In cells where glutamate increased the membrane conductance, there was a consistent increase in membrane current noise associated with the change in membrane current. This is shown in Fig. 5*A* where, along with the change in current induced at -65 mV when glutamate is applied to the cell, we also show a record of the same current high-pass filtered at 5 Hz (8-pole, Butterworth). As the current increases, so does the noise. The current noise increase is presumably due to the glutamate-induced opening and closing of ion channels.

Fig. 5*B* shows the variance of the glutamate-induced current fluctuations as a function of the mean glutamate-induced current flowing, during the period when the current was changing at the onset of the response (filled circles) and during the plateau

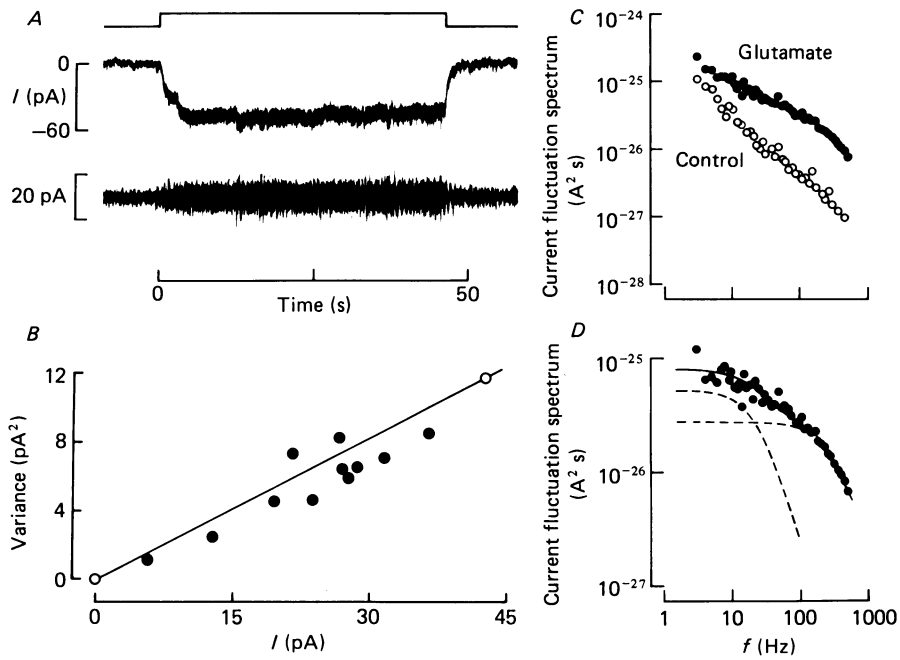

Fig. 5. *A*, current (middle trace) induced in a bipolar cell at −65 mV by ionophoretically applied glutamate (timing shown by upper trace: the ionophoretic current was switched from +10 to −10 nA to eject drug). The ionophoretic pipette was repositioned twice during the onset of the response and during the response plateau, giving small discontinuities in the current record. Lower trace: a higher gain current record high-pass filtered (5 Hz, 8-pole, Butterworth) to show the noise increase induced by the drug. Both records low-pass filtered (8-pole, Butterworth) at 250 Hz. Solution E in the pipette. *B*, variance of the glutamate-induced current in the range 2–1000 Hz, as a function of the glutamate-induced current. ○, values obtained from 15 s of data before the drug was applied (point at origin) and 19 s of data during the response plateau. ●, values obtained from 0·5 s bins during the onset of the response. Line through the points was calculated by linear regression with points weighted by their sample time. Slope of the line is 0·28 pA. *C*, spectrum of the current before and during glutamate application. Series resistance in this cell would give 1-pole filtering with a half-power frequency of 1024 Hz (so points above 500 Hz are not shown) – this leads to underestimating the power by 20 % at 500 Hz and 9 % at 300 Hz. *D*, difference between the spectra in *C*. Continuous line is the sum of the two Lorentzian components shown as dashed lines. Lower-frequency component has $G(0) = 0{\cdot}053$ pA², $f_c = 22{\cdot}4$ Hz; high-frequency component has $G(0) = 0{\cdot}028$ pA², $f_c = 275$ Hz.

of the response (open circles). The variance is approximately proportional to the mean current flowing, implying (Colquhoun & Hawkes, 1977) that the probability of channel opening is low. In this situation, if we assume that there is only one type of glutamate-gated channel present, with only one open state, we can take the ratio of the variance to the mean current to obtain the current flowing through a single channel opened by glutamate (see Methods). The slope of the linear regression line in Fig. 5*B* is 0·28 pA. After correction for variance lost below 2 Hz and above 1000 Hz (see Methods), this becomes 0·32 pA, implying a single-channel conductance of 6·06 pS for a reversal potential of −12 mV. Thus, to produce the current change

of 46 pA in Fig. 5*A*, approximately 144 channels must be open at any time (and since the probability of opening is low, there must be far more channels than this actually in the cell membrane). In six cells studied with 30 mM-Cl^- in the patch pipette (three cells with solution C and three cells with solution E), the average single-channel conductance found in this way was $5{\cdot}4 \pm 1{\cdot}3$ pS, roughly twice the value found for the channels opened by glutamate in goldfish horizontal cells (Ishida & Neyton, 1985) but much smaller than the 120 pS glutamate-gated channel in locust muscle (Anderson, Cull-Candy & Miledi, 1978). There was no significant difference between the values obtained with low or high internal calcium concentration (solutions C or E, respectively).

Fig. 5*C* shows the power spectrum of the membrane current fluctuations obtained before glutamate was applied, and during the plateau of the glutamate response in Fig. 5*A*. The difference between these two spectra is shown in Fig. 5*D*. The spectrum of the glutamate-induced noise could not be fitted by a single Lorentzian curve of the form:

$$G(0)/[1+(f/f_c)^2], \tag{1}$$

where f is the frequency, G(0) is the zero-frequency asymptote of the function, and f_c is the half-power frequency. To fit the spectra in all of the cells on which noise analysis was done, a sum of two Lorentzian terms (with different half-power frequencies) was necessary. The two Lorentzian spectra used to fit the data in Fig. 5*D* are shown as dashed lines in the Figure, with their sum shown as the continuous curve through the points. For six cells studied with 30 mM-Cl^- in the patch pipette at potentials between -46 and -65 mV, the half-power frequencies of the low- and high-frequency Lorentzian spectra were, on average, $f_c = 14{\cdot}0 \pm 6{\cdot}0$ Hz for the low-frequency component and $f_c = 205 \pm 60$ Hz for the high-frequency component. On average, the noise variance in the low-frequency component was one quarter ($0{\cdot}24 \pm 0{\cdot}15$) of that in the high-frequency component.

If there is only one type of glutamate-gated channel in these cells, a spectrum fitted by the sum of two Lorentzian curves is consistent with a kinetic scheme for channel opening in which there are three states (Colquhoun & Hawkes, 1977), for example:

$$\underset{\text{closed}}{\mathrm{T} + \mathrm{R}} \underset{k_2}{\overset{k_1}{\rightleftharpoons}} \underset{\text{closed}}{\mathrm{TR}} \underset{\alpha}{\overset{\beta}{\rightleftharpoons}} \underset{\text{open}}{\mathrm{TR}^*}. \tag{2}$$

In this scheme, T represents the transmitter, glutamate, and R represents the receptor complex which is initially closed and can only open when it has bound transmitter. The parameters k_1, k_2 and α, β are rate constants for transmitter binding and dissociation, and for channel opening and closing. If one of these pairs of rate constants were much faster then the other (for example, if transmitter binding and dissociation were very quick compared to the subsequent opening and closing of the channel, as assumed by Anderson & Stevens (1973) for the acetylcholine-gated channel at the neuromuscular junction), then two of the states in scheme (2) become indistinguishable, and a single Lorentzian spectrum is predicted (Colquhoun & Hawkes, 1977). Since we never found that a single Lorentzian spectrum would fit the data, we can rule out the possibility that there are only two kinetically distinct states.

So far, however, we have assumed that there is only one type of glutamate-gated

channel present in the cell membrane. Another interpretation of the two Lorentzian spectrum is that there are two types of glutamate-gated channel in the membrane, each with two kinetically distinct states, contributing two Lorentzian components with different half-power frequencies. We have no evidence to select or reject this hypothesis in favour of the preceding discussion in terms of one class of channel with three distinct states. Similar conclusions have been reached for glutamate-induced currents in cerebellar granule cells (Cull-Candy & Ogden, 1985).

Voltage noise produced by glutamate in hyperpolarizing bipolar cells

By making simple assumptions, it is possible to estimate the amount of voltage noise that glutamate, released from photoreceptors, induces in hyperpolarizing bipolar cells in the intact retina in the dark. This can be calculated knowing neither the concentration of glutamate reaching the bipolar cells in the intact retina nor the number of glutamate-gated channels present on the cells, if the probability of channel opening is low. To do this, we first calculate the amount of filtering of glutamate-induced current fluctuations that is performed by the bipolar membrane capacitance in the conversion of current into voltage in these cells. This is done by multiplying the spectrum of current fluctuations (e.g. Fig. 5*D*) by a Lorentzian spectrum with a filtering time constant of 2·7 ms (the membrane time constant measured for slice bipolars, described below), and calculating the effective current variance as the area under this new spectrum. For six cells, the filtered variance was a fraction $F = 0{\cdot}35 \pm 0{\cdot}09$ of the unfiltered variance. If the probability of glutamate-gated channels being open is low, the unfiltered current variance associated with these channels is (Colquhoun & Hawkes, 1977):

$$\text{current variance} = I i_1, \tag{3}$$

where I is the mean glutamate-evoked current and i_1 is the current flowing through an open channel. At the dark potential, $E_d = -45$ mV, the value of i_1 calculated from the mean single-channel conductance given above is 0·18 pA. The variance in membrane voltage, after filtering by the membrane capacitance, is therefore:

$$\text{voltage variance} = F I i_1 R_d^2, \tag{4}$$

where R_d is the cell's input resistance in the dark. We set $R_d = 120$ MΩ, the mean value we found for depolarizing bipolar cells in retinal slices, which is similar to the value found by Wu (1986) for hyperpolarizing bipolar cells in salamander retina, and comparable to the input resistance of hyperpolarizing bipolar cells in the intact turtle retina (Ashmore & Copenhagen, 1983). The glutamate-evoked current flowing at the dark potential can be shown to be:

$$I = (E_0 - E_d)(E_d - E_{rev})/[R_d (E_0 - E_{rev})], \tag{5}$$

where E_{rev} is the reversal potential of the glutamate-gated current ($E_{rev} = -12$ mV), and E_0 is the cell's membrane potential when the glutamate-gated channels are all closed. Taking $E_0 = -70$ mV (the voltage at the peak of the bipolar cell light response) gives $I = 119$ pA. The voltage variance from eqn. (4) is thus 0·106 mV², i.e. a standard deviation of 326 μV.

This value will be an underestimate of the true voltage variance if some glutamate-gated channels remain open in bright light so that E_0 is more negative than -70 mV. Conversely, it will be an over-estimate if the channel open probability p is not low in the dark: in this case eqn. (3) must be replaced by eqn. (7) (see below), so that the variance will be smaller by a factor of $(1-p)$. In either case, the correction is unlikely to be large, for the following reasons. For the first effect, even taking $E_0 = -100$ mV only makes the voltage variance 44% greater than the value quoted above. For the second effect, the fact that hyperpolarizing turtle bipolar cells can be depolarized by up to 25 mV from the dark potential at the offset of a prolonged bright flash of light (Ashmore & Copenhagen, 1983) – an effect attributed to a depolarization in cones transmitted synaptically (Schwartz, 1974) – suggests that p is small in the dark: if E_0 is -70 mV and we consider the worst case where p must be 1 to depolarize the cell by 25 mV from $E_d = -45$ mV, one can calculate that $p = 0{\cdot}12$ at the dark potential. The voltage variance would thus be smaller than that calculated above by a factor of $1-p = 0{\cdot}88$. Taking into account these two possible corrections, we predict the voltage noise will have a standard deviation between 305 and 390 μV.

Noise associated with the glutamate-induced conductance decrease

In cells where glutamate decreased the conductance, there was a pronounced reduction of current noise associated with this decrease (Fig. 6*A*). This result immediately rules out the simplest model for how glutamate closes ionic channels to decrease the conductance, i.e. by analogy with scheme (2) above, a scheme in which the transmitter binds to a receptor associated with the open channel and the channel can then close:

$$\mathrm{T} + \underset{\text{open}}{\mathrm{R}^*} \rightleftharpoons \underset{\text{open}}{\mathrm{TR}^*} \rightleftharpoons \underset{\text{closed}}{\mathrm{TR}}, \tag{6}$$

where T and R denote transmitter and receptor, and the asterisk implies the channel is open. This scheme is ruled out for the following reason. In general, the current variance associated with the transmitter-gated channels is given by (Colquhoun & Hawkes, 1977, eqn. (55)):

$$\text{current variance} = Ni_1^2\, p(1-p), \tag{7}$$

where N is the number of channels, i_1 is the current that flows through an open channel, and p is the probability of a channel being open. On scheme (6) above, if there is no transmitter present there can be no channels closed and the open probability must be $p = 1$. Thus, the variance contributed by these channels is 0, and when transmitter is added, decreasing p, the noise variance should *increase*. The fact that the variance *decreases* when the channels are closed by transmitter implies that the open probability is less than 0·5 even in the absence of transmitter.

The variance of the glutamate-modulated noise was found to be proportional to the current flowing through the channels which are closed by glutamate (Fig. 6*B*). This suggests that the probability of channels being open is low even in the absence of glutamate, and we are examining the low probability linear asymptote of the parabolic dependence on p in eqn. (7).

If we assume that there is only one type of channel closed by glutamate, with only one open state, then the slope of the straight line in Fig. 6*B* gives the current flowing through each of the open channels which are closed by glutamate. For Fig. 6*B* this value was 0·6 pA (after correction for variance lost at low and high frequencies, as described in Methods), giving a single-channel conductance of 14·1 pS for a reversal potential of $-13{\cdot}3$ mV. To produce the total current change of 7·2 pA in Fig. 6*A*,

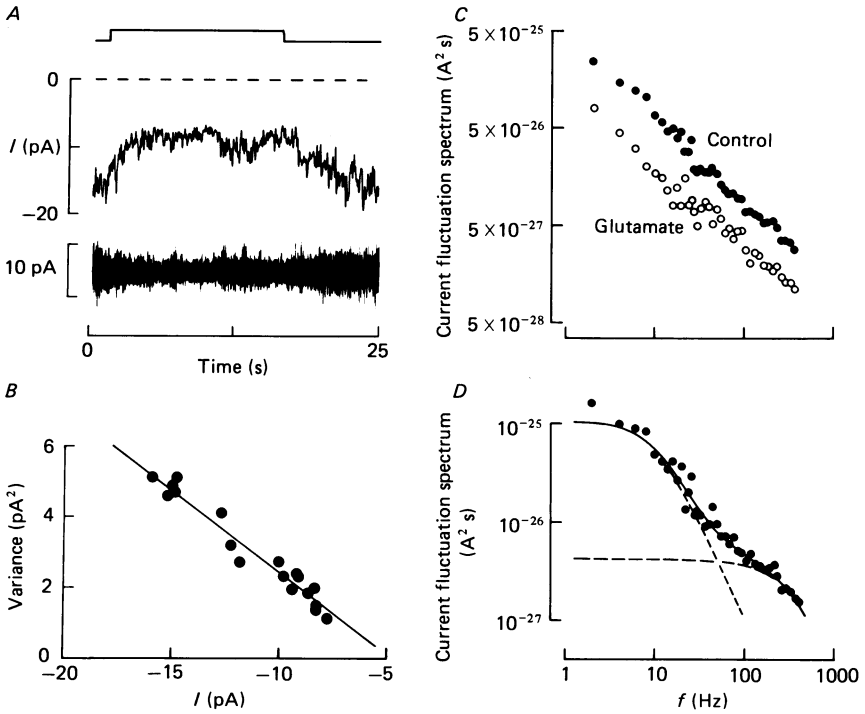

Fig. 6. *A*, current (middle trace) induced in an isolated bipolar cell at −56 mV by 1 mM-glutamate, applied at timing shown by the upper trace. Solution F in the pipette. Current record low-pass filtered (8-pole) at 10 Hz. Dashed line shows zero current through the pipette. Lower trace shows noise changes occurring during the response (filtered at 5 Hz high pass and 500 Hz low pass). *B*, variance of the current between 2 and 500 Hz as a function of membrane current during the response of *A*. Each point was obtained from 1·5 s stretches of data. The linear regression line has a slope of 0·46 pA. *C*, spectrum of the current fluctuations before and during glutamate application. Series resistance for this cell would give 1-pole filtering with a half-power frequency of 700 Hz. *D*, difference between the spectra in *C*. Continuous line is the sum of the Lorentzian components (dashed lines) with parameters: $G(0) = 0{\cdot}103$ pA², $f_c = 10{\cdot}2$ Hz and $G(0) = 0{\cdot}0041$ pA², $f_c = 290$ Hz. The spectra shown in *C* and *D* have been corrected for the effect of high-pass filtering at 2 Hz.

twelve of these channels must be closed at any time during the plateau of the response. On average, in three cells studied with 24 mM-Cl^- in the patch pipette (solution F of Table 1) the single-channel current was $0{\cdot}45 \pm 0{\cdot}13$ pA at −56 mV, giving a single-channel conductance of $10{\cdot}6 \pm 3{\cdot}1$ pS. Similar single-channel currents were obtained for cells studied with 100 mM-internal chloride (four cells with solution A).

The spectrum of the glutamate-suppressed noise (Fig. 6*C* and *D*) could not be fitted by a single Lorentzian spectrum, although the sum of two Lorentzian spectra gave a reasonable fit. In three cells studied at −56 mV (with 24 mM-Cl^- in the pipette), the average values of the Lorentzians' half-power frequencies were $f_c = 8{\cdot}3 \pm 2{\cdot}0$ Hz for the low-frequency component, and $f_c = 185 \pm 93$ Hz for the high-frequency component. On average, the variance in the low-frequency component was about one and a half times ($1{\cdot}6 \pm 0{\cdot}8$) that in the high-frequency component. Similar results were obtained for four cells with 100 mM-Cl^- in the pipette.

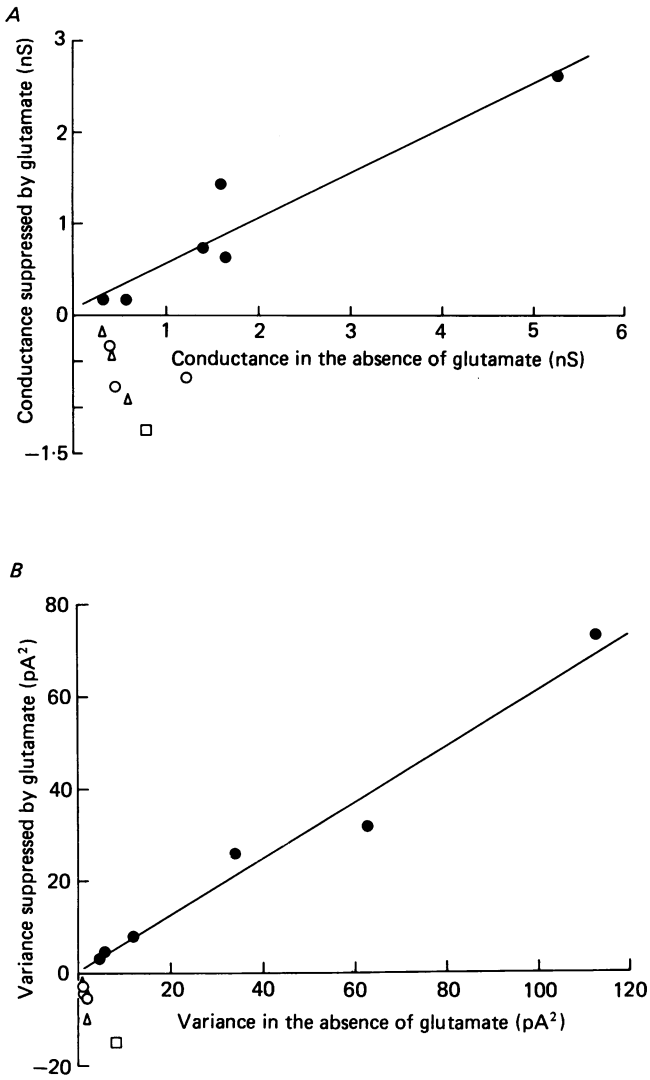

Fig. 7. Comparison of the conductance and current noise change induced by glutamate with the conductance and noise in the absence of glutamate, in cells which were sufficiently stable to allow accurate noise measurements to be made. *A*, conductance suppressed by glutamate plotted against cell conductance in the absence of glutamate (this includes the conductance of the seal between the electrode and the cell membrane). Data above the abscissa (●) are for conductance-decrease cells to which 1 mM-glutamate was applied. Data below the abscissa (with a negative value of conductance suppressed, i.e. a conductance increase) are for conductance-increase cells studied with glutamate applied by ionophoresis (△), or by superfusion at 250 μM (□) or 1 mM (○). Straight-line fit has a slope of 0·5. *B*, noise variance suppressed by glutamate in the frequency range 0–400 Hz for conductance-decrease cells (above the abscissa) and conductance-increase cells (below the abscissa, where a negative value of noise suppressed implies a noise increase). Symbols as in *A*. Membrane potentials between −45 and −65 mV. Straight-line fit has a slope of 0·62. The conductance-decrease cells with the smallest responses to glutamate had values of conductance and noise in the absence of glutamate similar to those found for conductance-increase cells. Conductance-decrease cells showing larger glutamate responses had larger initial conductance and noise values.

The magnitude of the noise decrease induced by glutamate varied considerably between cells, and was loosely correlated with the initial current noise in the cell (Fig. 7*B*), in the same way as the magnitude of the glutamate-induced conductance decrease was loosely correlated with the cell's conductance in the absence of glutamate (Fig. 7*A*). In cells where glutamate increased the membrane conductance, the initial conductance and current noise tended to be lower than for conductance-decrease cells. These data, together with the fact that the majority of the cells did not respond to glutamate at all, suggest that the proportion of glutamate-sensitive channels surviving the cell isolation procedure is rather variable and that, for presumed depolarizing bipolar cells, the glutamate-sensitive conductance and current noise can be a large fraction of the total cell conductance and current noise.

Voltage noise produced by glutamate in depolarizing bipolar cells

As for hyperpolarizing bipolar cells above, to estimate the contribution to the membrane voltage noise of the channels closed by glutamate in depolarizing bipolar cells, we mimicked the effect of filtering by the membrane capacitance by multiplying noise spectra like those in Fig. 6*D* by a Lorentzian spectrum with a time constant of 2·7 ms. For seven cells, the current variance after filtering was a fraction $F = 0{\cdot}63 \pm 0{\cdot}09$ of the unfiltered variance. Less variance is filtered out than for conductance-increase cells because a larger proportion of the current variance is at low frequencies for the channels closed by glutamate (compare Figs. 5*D* and 6*D*). Since the open probability of the channels closed by glutamate is low (see above), the voltage variance due to these channels in the dark is given by (cf. eqn. (4)):

$$\text{voltage variance} = FIi_1 R_d^2, \tag{8}$$

where R_d is the cell input resistance in the dark, i_1 is the current flowing through an open channel (0·36 pA at a dark potential of −45 mV), and I is the mean current flowing through those channels that remain open in the presence of the transmitter released tonically by photoreceptors in the dark.

The fraction of channels that remain open in the dark is unknown, though two lines of evidence suggest that they are not all closed. First, depolarizing photoreceptors, and thereby increasing the amount of transmitter they release, hyperpolarizes depolarizing bipolar cells from their dark potential: when cones are depolarized from their dark potential following a bright flash, depolarizing bipolar cells can hyperpolarize by at least 8 mV (in turtle: Schwartz, 1974; and in dogfish: Ashmore & Falk, 1980); likewise, injection of depolarizing current into rods in retinal slices can hyperpolarize depolarizing bipolar cells by at least 5 mV (in axolotl: Attwell, 1986). Secondly, application of the glutamate analogue 2-amino-4-phosphonobutyric acid can hyperpolarize depolarizing bipolar cells by 20 mV, presumably by closing the same channels as glutamate (in dogfish: Shiells *et al.* 1981). If we assume, as for hyperpolarizing bipolar cells (see p. 140), that the membrane potential of these cells when all the glutamate-gated channels are closed is $E_0 = -70$ mV, then in the same way as for hyperpolarizing bipolar cells we can calculate from eqn. (5) (using $E_{rev} = -13$ mV and $R_d = 120$ MΩ) that the current flowing through the channels that remain open at the dark potential ($E_d = -45$ mV) is $I = 117$ pA. With this value of I, and the values of i_1 and F given above, eqn. (8) predicts a voltage variance of

0·36 mV^2, i.e. a standard deviation of 600 μV. This is larger than the value estimated for hyperpolarizing bipolar cells, because of the larger conductance of the channels closed by glutamate and because less current variance is filtered out by the membrane capacitance for conductance-decrease than for conductance-increase cells.

If E_0 is more positive than −70 mV, the fraction of channels open in the dark, and hence the voltage noise, will be lower. However, even taking E_0 as positive as −50 mV (i.e. as positive as possible for consistency with the 5 mV hyperpolarization evoked by rod depolarization described above), gives a standard deviation of 340 μV.

Kinetic model for the glutamate-induced conductance decrease

As stated above, the fact that the channels' open probability is less than 0·5 in the absence of glutamate rules out the simplest three-state scheme conceivable for the action of glutamate on the channel (scheme (6) above). A simple alternative scheme, which is consistent with the open probability being less than 0·5, and being decreased when glutamate is applied, is shown here:

$$\underset{\text{open}}{\mathrm{R}^*} \underset{\beta}{\overset{\alpha}{\rightleftharpoons}} \underset{\text{closed}}{\overset{\mathrm{T}}{\mathrm{R}}} \underset{k_2}{\overset{k_1}{\rightleftharpoons}} \underset{\text{closed}}{\mathrm{TR}}. \tag{9}$$

In the absence of transmitter (T), the receptor-channel complex can exist in two states, open (R*) and closed (R), and the fraction of channels which are open is $\beta/(\alpha+\beta)$. Thus, if $\beta < \alpha$ the open probability is less than 0·5. When transmitter is present it is postulated to combine with the closed form of the channel, driving it into another closed state (TR).

The noise spectrum predicted for scheme (9), however, is not in agreement with that found experimentally. In the absence of transmitter, only two states are possible in scheme (9), giving rise to current noise with a single Lorentzian power spectrum (with half-power frequency $(\alpha+\beta)/2\pi$). When a non-saturating level of glutamate is applied, all three states in scheme (9) are possible and the current noise spectrum would be the sum of two Lorentzian curves (Colquhoun & Hawkes, 1977). In the presence of excess transmitter (when all channels are closed) there would be no current noise contributed by the glutamate-gated channels. Thus, the experimentally observed difference spectrum of the glutamate-sensitive noise (spectrum with no drug present minus spectrum in the presence of glutamate as plotted in Fig. 6*D*) would consist of one Lorentzian curve for a saturating level of glutamate, and would be the difference between one Lorentzian curve and the sum of two Lorentzian curves for a non-saturating glutamate level. By plotting these predicted difference spectra, we found that none of them could, even roughly, fit our experimentally observed difference spectra (Fig. 6*D*), which can be approximately described by the sum of two Lorentzian curves.

A simple modification of scheme (9), however, can predict a glutamate-induced noise decrease which has a difference spectrum described by the sum of two Lorentzian curves. A four-state scheme such as scheme (10):

$$\underset{\text{closed}}{\mathrm{R}'} \rightleftharpoons \underset{\text{open}}{\mathrm{R}^*} \rightleftharpoons \underset{\text{closed}}{\overset{\mathrm{T}}{\mathrm{R}}} \rightleftharpoons \underset{\text{closed}}{\mathrm{TR}}, \tag{10}$$

would generate a two Lorentzian spectrum for the current noise in the absence of transmitter, and in the presence of excess glutamate all the channels would be closed and contribute no noise. The difference spectrum would thus be the sum of two Lorentzian curves. Other, more complex modifications of scheme (9) can also result in two Lorentzian spectra.

The light-induced synaptic current in depolarizing bipolar cells

To check whether the glutamate-induced currents in isolated bipolar cells resembled the synaptic currents evoked by the transmitter released from photoreceptors, and to investigate whether there were any voltage-gated currents in bipolar cells in the retina that were lost during the procedure for cell isolation, we studied membrane currents in bipolar cells in retinal slices (see Methods).

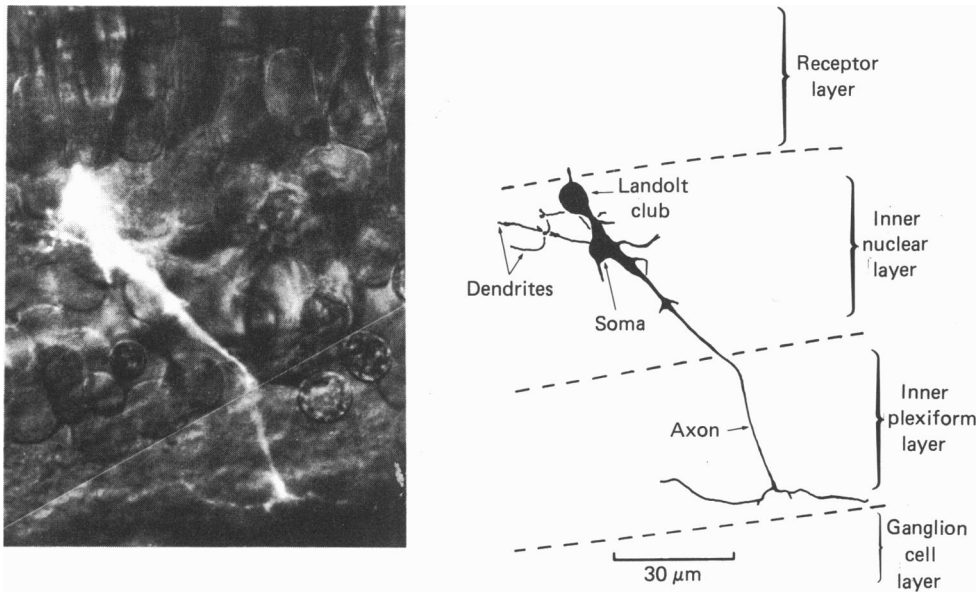

Fig. 8. A depolarizing bipolar cell in a living retinal slice, filled with the fluorescent dye Lucifer Yellow, which was included in the patch pipette used to voltage clamp the cell. The long photographic exposure needed to visualize the axon and some of the dendritic processes of the cell has resulted in the cell body and Landolt club being over-exposed. The drawing to the right makes the Lucifer-Yellow-filled processes easier to identify. It was made by tracing several photographs taken with different exposure times with only the exciting light for the fluorescent dye illuminating the preparation. The axon terminals of the cell are in the inner half of the inner plexiform layer, as expected for a depolarizing bipolar cell (Lasansky, 1978).

Patch clamping in retinal slices was much more difficult than patch clamping isolated cells for two reasons. First, access of the patch pipette to the cell membrane was often hindered by other cells and debris on the surface of the slice, which often prevented giga-seal formation. Secondly, the image of the slice preparation and pipette obtained with our infra-red viewing system (used to preserve the cells' light responses) was much less clear than when viewing isolated cells with visible light

directly through the microscope. We recorded from eighty-four cells, of which eight were positively identified as depolarizing bipolar cells, one of which is shown filled with Lucifer Yellow in Fig. 8. No cells were unambiguously identified as hyperpolarizing bipolars, although micro-electrode studies (S. Borges & M. Wilson, unpublished) reveal that a significant proportion of bipolar cells in the axolotl retina are

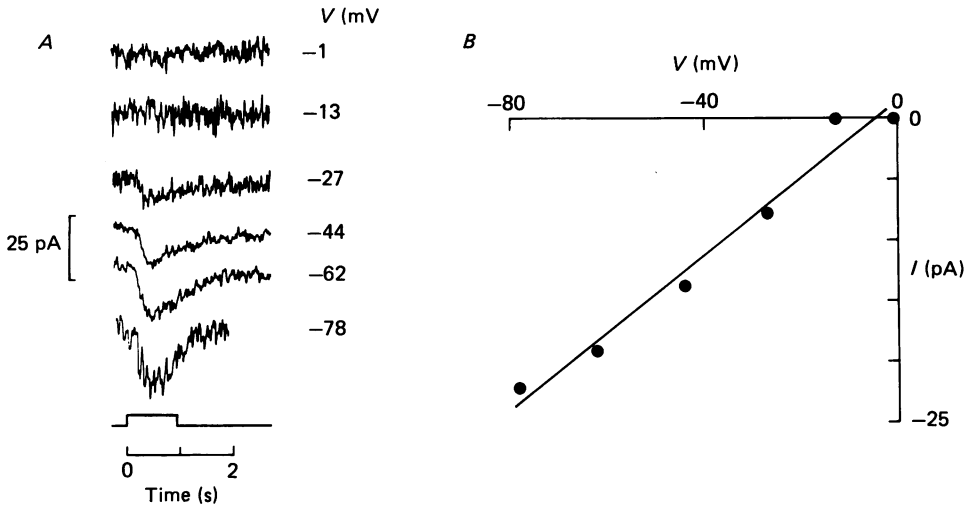

Fig. 9. *A*, current evoked in a depolarizing bipolar cell in a retinal slice by illumination with an 80 μm spot of 520 nm light (3460 photons μm^{-2} s^{-1}) centred on the photoreceptors above the bipolar cell's dendritic field. Voltage-clamp potentials shown beside each trace. (Solution E in the pipette.) *B*, peak current–voltage relation for the data in *A*. Linear regression line has a reversal potential of −5 mV.

hyperpolarizing cells. It is more difficult to identify hyperpolarizing bipolar cells than depolarizing bipolar cells in retinal slices, because there is the possibility of confusion with horizontal cells, which also hyperpolarize in response to light and have cell bodies at the outer part of the inner nuclear layer.

Resting potentials measured in depolarizing bipolar cells had a mean value of -28 ± 22 mV. The membrane capacitance was $21{\cdot}4 \pm 11{\cdot}0$ pF, i.e. roughly twice the value found for isolated cells. At potentials negative to −40 mV, the current–voltage relation of slice bipolars was roughly ohmic, with a mean input resistance of 120 ± 80 MΩ. The average value of the membrane time constant was 2·7 ms. Depolarization past −30 mV evoked a fast time-dependent increase in outward current which then decreased more slowly, as for isolated cells (Fig. 2), in four of the eight depolarizing bipolar cells studied. The other four cells showed time-independent, roughly ohmic responses to voltage-clamp steps between −80 and +20 mV (i.e. similar to the 10% of isolated bipolar cells showing no time-dependent current, but with a lower input resistance).

To study the synaptic current produced by the photoreceptors, with minimal contamination from horizontal cell input, we illuminated the receptors above the bipolar cell being recorded from with an 80 μm diameter light spot. This diameter

is well within the receptive field centre of the bipolar cell, and a spot of this diameter will not significantly polarize horizontal cells.

Fig. 9 shows the light-induced synaptic current evoked in a depolarizing bipolar clamped to various potentials. The inward current generated by light was reduced at less negative potentials (five cells), and the peak current–voltage relation of Fig. 9*B* extrapolates to a reversal potential around −5 mV (mean value −2·5±4·2 mV), similar to the reversal potential for the channels closed by glutamate

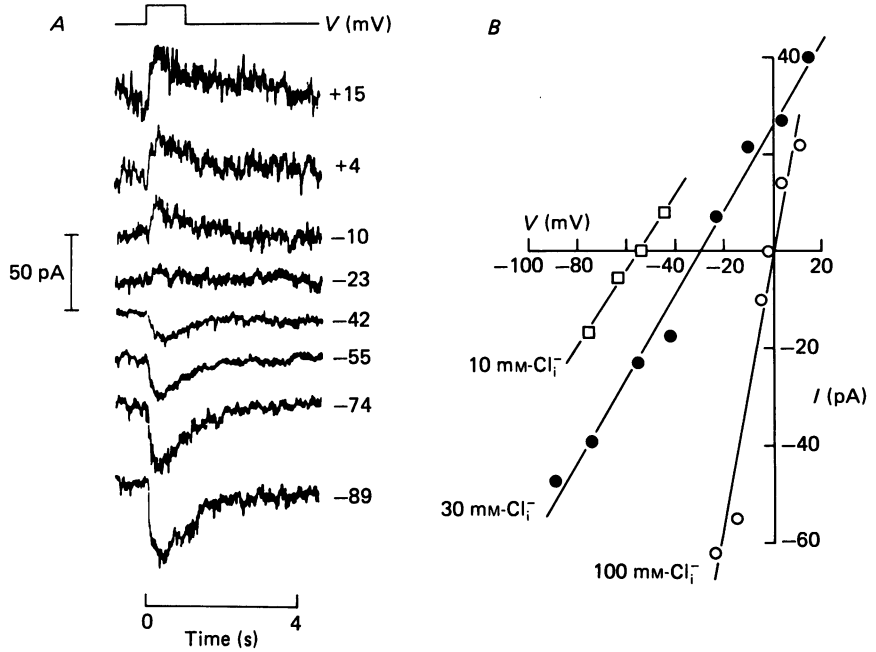

Fig. 10. Currents induced in an isolated bipolar by ionophoretically applied GABA (timing shown by upper trace, ionophoretic current was switched from −10 to +10 nA for ejection), using a patch pipette containing 30 mM-Cl_i^- (solution B). Voltage-clamp potentials shown by each trace. *B*, current–voltage relations for the data in *A* (●) and for two other cells studied using 10 mM-$Cl^-{}_i$ (□) or 100 mM-Cl_i^- (○) in the patch pipette.

in isolated bipolar cells. We were never able to reverse the light-induced current, even polarizing as positive as +25 mV. This may reflect voltage non-uniformity in the bipolar cell dendrites between the soma and the site of synaptic input, which will be worse at more positive potentials because of the outward rectification in the cell's current–voltage relation (Fig. 2).

The data in Fig. 9*A* show that the current modulated by the photoreceptor transmitter has a reversal potential positive to the physiological response range, and thus that the transmitter acts by closing ionic channels. We presume that these are the same channels that are closed by glutamate in isolated bipolar cells.

Candidates for transmitters mediating lateral inhibition

Evidence reviewed in the Introduction indicates that GABA and glycine may mediate lateral inhibition from horizontal and amacrine cells onto bipolar cells. Of sixty-five isolated bipolar cells to which we applied GABA, thirty-two (49 %) showed a GABA-evoked current. Glycine evoked a current in twenty (87 %) of the twenty-three cells it was applied to. For three bipolar cells, both GABA and glycine were tested, and all three cells responded to both agents.

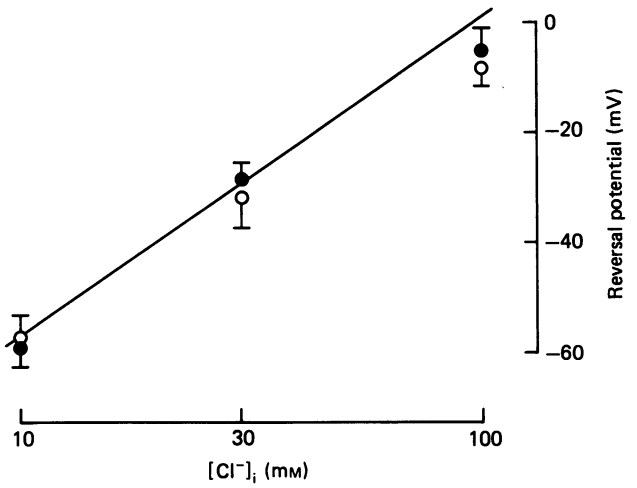

Fig. 11. Reversal potential of the currents induced by GABA and glycine, as a function of chloride concentration in the patch pipette. Line shows the Nernst equation $E_{Cl} = (RT/F) \ln ([Cl^-]_o/[Cl^-]_i)$ with $[Cl^-]_o$ (external chloride concentration) = 96·5 mM. Points show mean and standard deviation of the reversal potential in, for GABA, two, seven and five cells for 10, 30 and 100 mM-Cl_i^- respectively and for glycine, five, three and three cells for 10, 30 and 100 mM-Cl_i^-. ●, GABA; ○, glycine.

The GABA-induced current

Fig. 10*A* shows typical currents evoked in an isolated bipolar cell by iontophoretically applied GABA. GABA increases the membrane conductance. For this cell, which was studied with a patch pipette containing 30 mM-Cl^- (solution B), the reversal potential of the GABA-induced current was −29 mV. With 30 mM-Cl^- in the patch pipette (and hence presumably in the cell) and 96·5 mM-Cl^- in the external solution, the Nernst potential for chloride is −29 mV, suggesting that GABA opens chloride channels in these cells, as in other preparations (Hamill, Bormann & Sakmann, 1983).

This idea was tested further by studying the GABA-evoked current using patch pipettes containing either 100 or 10 mM-Cl^- (solutions A or D). Typical current–voltage data for the GABA-induced currents are shown in Fig. 10*B*. With 100 mM-Cl^- in the patch pipette the reversal potential is around 0 mV, while with 10 mM-Cl^- the reversal potential is near −55 mV. In Fig. 11 the average reversal potentials measured for cells with each of the three internal chloride concentrations are plotted as a function of chloride ion concentration. The straight line, on which the points

approximately fall, is the Nernst equation for chloride ions. We conclude that GABA opens chloride channels, although it is worth noting that there is a small, but significant, discrepancy from the Nernst prediction at high pipette chloride concentration. For seven cells studied with 30 mM-Cl^- solution in the patch pipette, the mean conductance induced by GABA was $1{\cdot}7 \pm 1{\cdot}1$ nS. Since this is greater than the

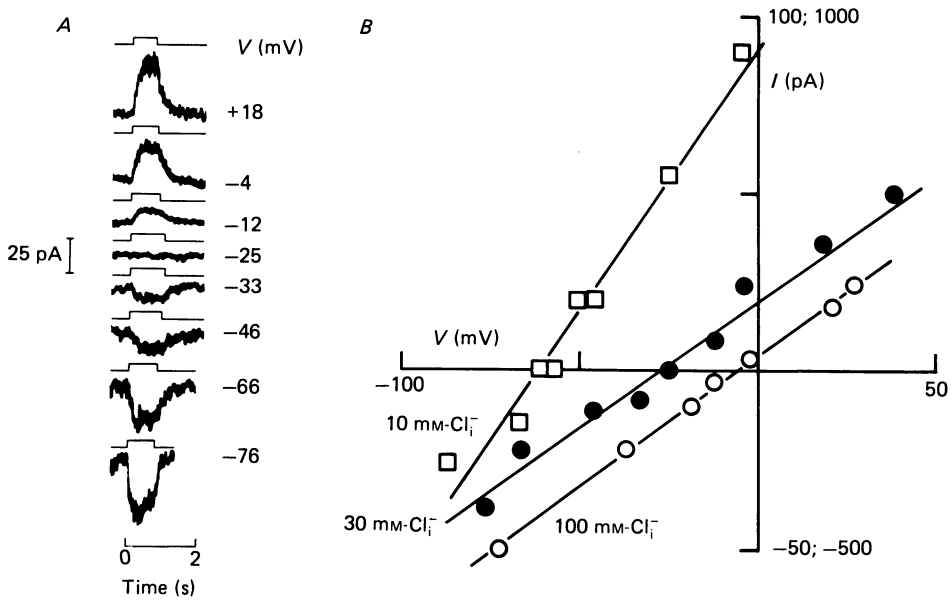

Fig. 12. *A*, current induced in an isolated bipolar cell by ionophoretically applied glycine (manually controlled timing shown above each trace, ionophoretic current switched from −10 to +10 nA for ejection, voltage-clamp potential shown by each trace), with 30 mM-Cl_i^- in the patch pipette (solution B). *B*, current–voltage data for the cell of *A* (●) and for two other cells studied with 10 mM-Cl_i^- (□) or 100 mM-Cl_i^- (○) solution in the pipette. The scale on the ordinate is ten times larger for the cell with 100 mM-Cl_i^-, because this cell was particularly responsive to glycine.

conductance in the absence of GABA, the GABA-gated current is capable of significantly controlling the cells' membrane potential. The data in Fig. 10*B* show a larger conductance when the internal chloride concentration, was larger, but this is a chance sampling of the data: for any particular value of $[Cl^-]_i$ there were large differences between cells in the magnitude of the GABA-induced conductance, and this variability prevented us from assessing the $[Cl^-]_i$ dependence of the conductance change.

The glycine-induced current

Glycine-induced currents, studied with the same protocol as used for GABA, are shown in Fig. 12. The data in Fig. 12*A* for 30 mM-Cl^- solution in the patch pipette, and the current–voltage relations for 10 and 100 mM-Cl^- in Fig. 12*B* are consistent with glycine opening chloride channels. The dependence of the reversal potential of the glycine-evoked current on pipette chloride concentration (Fig. 11) fits the Nernst

equation reasonably well, but again shows a slight deviation at 100 mM-Cl^-. In six cells studied with 30 mM-Cl_i^- (solution B), the mean conductance increase produced by glycine was $1{\cdot}7 \pm 1{\cdot}7$ nS.

Effects of bicuculline and strychnine

The actions of GABA and glycine were antagonized by the blocking agents bicuculline and strychnine respectively (Fig. 13). For these experiments double-barrelled ionophoretic pipettes were used, one barrel filled with the transmitter and

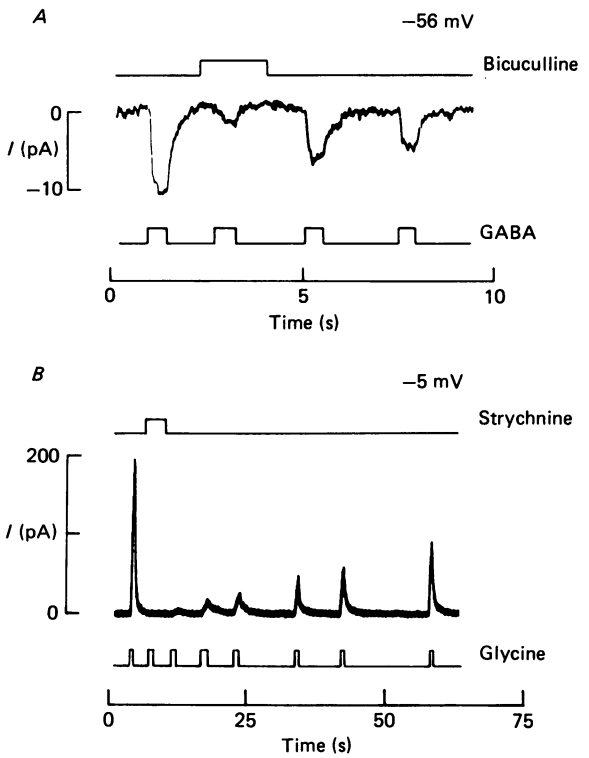

Fig. 13. *A*, effect of ionophoretic bicuculline application (timing shown by top trace, ionophoretic current switched from −6 to +39 nA for ejection) on the membrane current (middle trace) evoked at −56 mV by ionophoretically applied GABA (bottom trace, ionophoretic current switched from −10 to +10 nA for ejection). Solution B (30 mM-Cl^-) in the patch pipette. *B*, effect of ionophoretically applied strychnine (current switched from −6 to +40 nA for ejection) on the current evoked at −5 mV (i.e. above the reversal potential) by ionophoretically applied glycine (current switched from −10 to +10 nA for ejection). Solution D (10 mM-Cl^-) in the patch pipette. Note that the current pulses applying glycine were made longer during strychnine application, in an attempt to produce a glycine response when strychnine had slowed the rising phase of the response.

the other filled with the blocking agent under study. Fig. 13*A* shows repeated applications of GABA evoking an inward current in a bipolar cell. When bicuculline was applied, the GABA response was greatly reduced and slowed in onset. On removal of the bicuculline the GABA response recovered, although not completely because

this cell showed desensitization during repeated applications of GABA (note that the last response is smaller than the penultimate response). This action of bicuculline is consistent with GABA acting on bipolar cells via $GABA_A$ receptors, i.e. the type of GABA receptor found to control chloride channels in other preparations (for a review, see Simmonds, 1983).

Fig. 13*B* shows a similar result for the effect of strychnine on the glycine response. The onset of the response is slower immediately after strychnine. It often took over 5 min for cells to recover completely from the effects of strychnine (even when perfusion ensured that no strychnine remained around the cell after 30 s), suggesting that the rate constant for strychnine dissociating from the receptor is low.

The fact that bicuculline and strychnine slow the rising phase of the GABA and glycine responses is consistent with these drugs acting as competitive receptor antagonists (which can be slowly displaced from the receptors by the normal agonist), rather than as blockers of the open chloride channels which would not affect the initial rate of rise of the response.

Estimation of the internal chloride concentration

For a few cells to which we applied GABA or glycine, we noticed that the reversal potential of the transmitter-induced current was initially at a different value from the value it finally assumed. For example, in one cell studied with 100 mM-Cl^- solution in the patch pipette the reversal potential of the glycine-induced current was initially −30 mV soon after obtaining a whole-cell clamp, but over a period of a few minutes moved to −8 mV. The pipette used for this cell had a particularly large series resistance (70 MΩ, corresponding to a large barrier for diffusion into the cell), and it seems likely that the reversal potential shift occurs as the 100 mM-Cl^- solution equilibrates with the cell interior, raising the internal chloride concentration. Similarly, for another cell, studied with 10 mM-Cl^- solution in the pipette, the reversal potential of the GABA response was initially −45 mV, but finally stabilized at −56 mV.

Since the GABA- and glycine-gated channels are chloride-specific (Fig. 11), we interpret these data to indicate that for the first cell E_{Cl}, the chloride reversal potential, was initially −30 mV or below (since some equilibration of the pipette solution with the cell would have occurred before the reversal potential was first measured), corresponding to $[Cl^-]_i < 29$ mM, while for the second cell E_{Cl} was initially −45 mV or above, implying $[Cl^-]_i > 16$ mM. Unfortunately, these cells were not tested with glutamate to identify them as depolarizing or hyperpolarizing cells, which may have different values for $[Cl^-]_i$ (see Discussion).

The precise calculation of the cell chloride concentration is complicated, however, by the fact that as the pipette solution diffuses into the cell a time-dependent tip potential will exist between the patch electrode and the cell. The exact magnitude of this tip potential is difficult to calculate, but if chloride and/or acetate ions in the electrode are replacing slower-diffusing intracellular anions, while the cations in the cell and in the electrode are of comparable mobility, the tip potential will make the cell potential more negative than the measured potential. Thus, the estimates of initial chloride concentration for the two cells above will be too high.

Noise associated with the responses to GABA and glycine

As well as increasing the membrane conductance, both GABA and glycine increased the noise in the membrane current. This is shown for GABA in Fig. 14*A*. Fig. 14*B* shows the variance of the GABA-evoked noise as a function of the mean current flowing. The continuous line in Fig. 14*B* is drawn through the points obtained during the slow recovery of the cell's current after the removal of GABA (filled circles). The variance is approximately proportional to the mean current, implying that the channel open probability is low. As for glutamate (see above), the ratio of the current variance to the mean current was used to obtain the current flowing through an open channel, and hence the single-channel conductance (assuming that all GABA-gated channels have the same conductance). For three cells studied with 30 mM-Cl^- in the pipette (solution B), the average single-channel conductance obtained in this way was $4{\cdot}4 \pm 2{\cdot}2$ pS. A similar analysis of glycine-induced current changes showed that the probability of channel opening was low, and gave an average conductance of $7{\cdot}5 \pm 2{\cdot}9$ pS for three cells studied with 30 mM-Cl^- in the pipette (solution B).

Fig. 14*C* shows the power spectrum of the current noise for the cell of Fig. 14*A* in the absence of GABA, and at the plateau of the response to GABA, after desensitization had occurred (see below). The difference between these spectra (Fig. 14*D*) was fitted by the sum of two Lorentzian curves, suggesting that either there is one type of channel present with three kinetically distinct states, or two types of channel with two distinct states each. For three cells studied with 30 mM-Cl^- in the pipette at -56 mV, the half-power frequencies of the low- and high-frequency Lorentzians were, on average, $f_c = 8{\cdot}3 \pm 2{\cdot}9$ Hz for the low-frequency component, and $f_c = 117 \pm 50$ Hz for the high-frequency component. Similarly, the spectra of glycine-evoked current fluctuations required the sum of two Lorentzian curves to fit them. For three cells studied with 30 mM-Cl^- in the pipette at potentials between -61 and -51 mV, the half-power frequencies were, on average, $f_c = 9{\cdot}35 \pm 5{\cdot}8$ Hz for the low-frequency component, and $f_c = 116 \pm 49$ Hz for the high-frequency component.

The responses of most cells to GABA and glycine desensitized. This is shown for GABA in Fig. 14*A*. The decrease in current response during prolonged drug application is unlikely to be due to a decrease in drug release from the ionophoretic pipette: the backing current applied before drug ejection depletes drug from the electrode tip, and when ejection is started, equilibration of the drug concentration in the electrode tip should lead, if anything to an *increase* in drug ejection with time (Dionne, 1976). We found that the spectrum of the drug-induced noise did not change shape significantly during desensitization (in the range 8–512 Hz where the spectral densities at the peak of the response could be measured accurately). In addition, as illustrated by the dashed line in Fig. 14*B*, the relationship between current variance and mean GABA-evoked current when the response to GABA is desensitizing (open circles in Fig. 14*B*) is linear, with the same slope as during the cell's recovery following GABA application (filled circles in Fig. 14*B*). When the probability of channel opening is low, eqn. (7) predicts a linear dependence of variance on the mean current flowing (with slope i_1), whether the mean current is altered simply by varying the

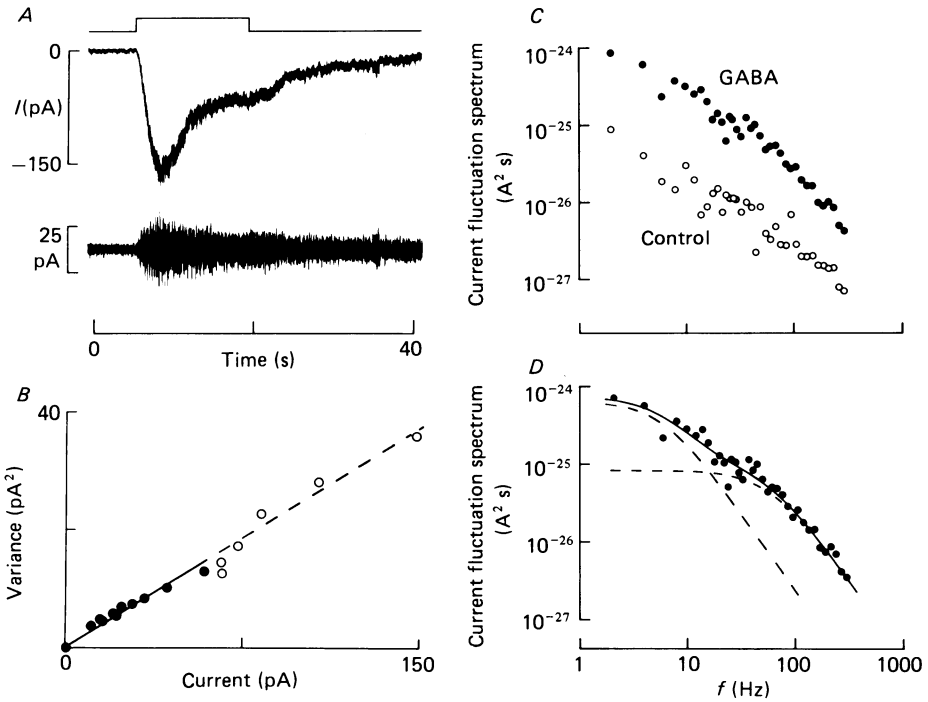

Fig. 14. GABA-induced current noise. *A*, ionophoretic application of GABA (top trace, ionophoretic current switched from −10 to +10 nA for ejection) to a cell studied with 30 mM-Cl^- in the pipette (solution B) evokes an inward current at −57 mV that desensitizes (middle trace, low-pass filtered (8-pole, Butterworth) at 500 Hz). The cell's membrane potential was changed before the current and noise had recovered completely to their pre-GABA levels. The lower trace, low-pass filtered at 500 Hz and high-pass filtered at 2 Hz (8-pole, Butterworth), shows the noise change on a larger scale. *B*, GABA-induced noise variance in the range 2–500 Hz as a function of GABA-induced current. Points were obtained from 2 s stretches of data during the application of GABA (○) and during the slow recovery following GABA application (●). Line was calculated by linear regression from the control data and the data obtained during recovery following GABA application and has a slope of 0·24 pA. Correcting for variance lost by filtering at 2 and 500 Hz (see Methods) and using the reversal potential of the GABA-evoked current in this cell gives an estimated single-channel conductance of 6·9 pS. *C*, spectrum of the current at the plateau of the response to GABA, and before GABA application. Series resistance for this cell would give 1-pole filtering with a half-power frequency of 600 Hz. *D*, difference between the spectra in *C*. Continuous line is the sum of Lorentzian components (dashed lines) with parameters: $G(0) = 0{\cdot}65$ pA², $f_c = 6{\cdot}1$ Hz; and $G(0) = 0{\cdot}085$ pA², $f_c = 60$ Hz. The shape of the noise spectrum did not change significantly during desensitization (see text). The spectra shown in *C* and *D* have been corrected for the effect of high-pass filtering at 2 Hz.

open probability, as presumably happens during the decay of the current after removal of GABA, or by varying the number of functioning channels (or both the number of channels *and* the open probability), as may happen during desensitization. The simplest interpretation of the results described here is that desensitization simply reduces the number of functioning channels without altering the noise contributed by non-desensitized channels. Similar results were obtained during the desensitization of responses to glycine (not shown).

DISCUSSION

Membrane currents and signal shaping in bipolar cells

In both isolated and slice bipolar cells of the axolotl, the membrane current–voltage relation is time independent and roughly ohmic between −30 and −70 mV, i.e. over most of the physiological response range of −25 to −70 mV. Thus, the bipolar cell light response is not significantly shaped by voltage-gated currents: differences in the wave form of the light response in photoreceptors and bipolar cells must be ascribed to filtering in the photoreceptor–bipolar synapse or to synaptic input from other cells. These bipolar cells differ, therefore, from rods and cones, where voltage-gated currents enhance the transience of the visual signal (Detwiler, Hodgkin & McNaughton, 1978; Attwell & Wilson, 1980; Attwell, Werblin & Wilson, 1982). They also differ notably from bipolar cells in the goldfish, which possess an inward current activated by hyperpolarization which will increase the transience of the visual signal (Kaneko & Tachibana, 1985).

In 90% of isolated bipolar cells and 50% of slice cells, depolarization beyond −30 mV activates a transient outward current. We have not carried out a full kinetic analysis of this current because its voltage range of activation is almost entirely outside the physiological range. We are uncertain whether the cells which showed no time-dependent current form a separate class of cells or are simply damaged in some way.

Bipolar cells in retinal slices had a capacitance which was roughly twice as large, and a resistance which was roughly ten times smaller than those of isolated cells. There are several likely reasons for this. First, the isolation procedure removes some of the cells' processes, thereby decreasing the total membrane area, the membrane capacitance and the total number of channels. Secondly, the existence of gap junctions between neighbouring bipolar cells (Wong-Riley, 1974), and the fact that the central receptive field of bipolar cells is larger than their dendritic field (Borges & Wilson, 1984; Hare, Capovilla & Owen, 1984), suggests that adjacent bipolar cells may be electrically coupled. In this case the apparent membrane capacitance would be greater than for single cells and the input resistance would be less. (There may also be substantial voltage non-uniformity on this account when voltage clamping the bipolar cell network at one point.) Finally, the input resistance of cells in the slice will be diminished by the effect of tonic synaptic input from other cells.

Identity of the photoreceptor transmitter

Evidence reviewed in the Introduction suggests several candidates for the photoreceptor transmitter. Of the five substances released from toad photoreceptors on depolarization, aspartate, *N*-acetylhistidine, cadaverine and putrescine had no effect on isolated bipolar cells, while glutamate induced a conductance increase in some cells and a conductance decrease in other cells. These results suggest that glutamate is the photoreceptor transmitter, consistent with the results of Lasater *et al.* (1984), Ishida *et al.* (1984) and Slaughter & Miller (1985). Glutamate may be the transmitter in both rods and cones, though we cannot rule out the possibility that (say) glutamate is the rod transmitter and another untested substance is the transmitter for cones.

Our finding that only a minority of isolated bipolar cells showed a response to glutamate is consistent either with glutamate channels being lost through amputation

of crucial parts of the cell membrane during the cell isolation procedure, or through disabling of the channels by the action of the proteolytic enzyme papain. Against these explanations must be set the observation that responding and non-responding cells are not morphologically distinguishable and there is no compelling reason why papain should affect some cells more than others. We cannot exclude the possibility that some bipolar cells receive input from photoreceptors via a transmitter other than glutamate and the four other substances tested (or that our cell isolation procedure *always* removed receptors to the four other substances).

The two effects of glutamate

The reversal potentials of the currents associated with the conductance increase and the conductance decrease induced by glutamate were approximately -12 mV, in agreement with data for the glutamate-activated channels in isolated horizontal cells (Ishida *et al.* 1984), and with estimates for the reversal potentials of the currents gated by the photoreceptor transmitter in hyperpolarizing and depolarizing bipolar cells in the intact retina (Toyoda, 1973; Ashmore & Falk, 1980). Thus, in the physiological potential range glutamate induces an inward current in some cells (conductance-increase cells), and an outward current in other cells (conductance-decrease cells). We postulate these two classes of cell to be hyperpolarizing and depolarizing bipolar cells, respectively (since hyperpolarization of photoreceptors by light suppresses transmitter release from their synaptic terminals).

The idea that the photoreceptor transmitter *closes* channels on depolarizing bipolar cells (Kaneko, 1971) was confirmed by recording the voltage dependence of the synaptic current evoked by light in depolarizing bipolar cells in retinal slices (Fig. 9).

Although the conductance increase and the conductance decrease induced by glutamate have the same reversal potential, and thus may be mediated by the same ionic species, several other properties of the responses differ, as follows.

(1) The glutamate receptors on presumed depolarizing bipolar cells seem to be less sensitive to glutamate than the receptors on presumed hyperpolarizing cells, and are detected more frequently if 1 mM rather than smaller concentrations of perfused glutamate is applied. This may account for the fact that Lasater *et al.* (1984), who used 100–500 μM-glutamate, found only bipolar cells for which glutamate increased the conductance among their isolated cells from skate retina. Although a glutamate concentration of 1 mM seems quite high, the acetylcholine concentration in the synaptic cleft at the neuromuscular junction is believed to rise to around 1 mM during synaptic transmission (Matthews-Bellinger & Salpeter, 1978).

(2) The onset of the glutamate-induced current was slower in presumed depolarizing than in presumed hyperpolarizing cells. A difference in the properties of the bipolar glutamate receptors (and their associated channels) has been suggested to underlie the slower impulse response for synaptic transmission from receptors to depolarizing bipolars than for transmission to hyperpolarizing bipolars (Ashmore & Copenhagen, 1980), and the slower over-all transmission from receptors to 'on' ganglion cells than to 'off' ganglion cells (Baylor & Fettiplace, 1977).

(3) Although we have not investigated the pharmacological properties of the glutamate responses in isolated bipolar cells, the work of others (Slaughter & Miller,

1981, 1983*b*, 1985) suggests that the receptors on depolarizing and hyperpolarizing cells are pharmacologically distinct.

Lateral inhibition

As might have been predicted from their effects on other cells, the transmitters believed to be involved in mediating lateral inhibition, GABA and glycine, open chloride channels in isolated bipolar cells. The smaller proportion of cells responding to GABA (49 %) than to glycine (87 %) may reflect a genuine physiological difference, or may be due to the cell isolation procedure degrading the GABA receptors more frequently. Wu (1986) finds that only 45–60 % of hyperpolarizing bipolar cells in the salamander retina have their receptive field inhibitory surround mediated by GABA and that only 60 % of horizontal cells accumulate GABA, suggesting that another transmitter, possibly glycine, mediates lateral inhibition onto the remaining bipolar cells. Since glycine responses were found in nearly all cells tested it is clear that bipolar cells can have both glycine and GABA receptors, and this was verified directly in three cells. Similarly, it seems likely that GABA and glycine receptors exist on the same cells as glutamate receptors.

The effect of GABA and glycine released onto bipolar cells from horizontal and amacrine cells in the retina will depend crucially on the chloride reversal potential in the bipolar cells. If the bipolar receptive field surround is produced mainly by direct input from horizontal (or amacrine) cells (Werblin & Dowling, 1969; Marc, Stell, Bok & Lam, 1978), rather than by GABA-mediated feed-back to cones (Baylor, Fuortes & O'Bryan, 1971; Attwell, Werblin, Wilson & Wu, 1983; Tachibana & Kaneko, 1984), then E_{Cl} must be above the resting potential in depolarizing bipolar cells (to produce a hyperpolarizing surround) and below the resting potential in hyperpolarizing bipolar cells. Miller & Dacheux (1983) have presented evidence that this may be the case.

Voltage noise in bipolar cells

From the membrane current noise in isolated cells identified from their response to glutamate as hyperpolarizing bipolars (in which the glutamate-gated channels are closed in the absence of transmitter), we estimated that the non-synaptic membrane currents in bipolar cells produce voltage noise in the dark with a standard deviation of 100–300 μV. We have also shown that the channels opened (on presumed hyperpolarizing bipolar cells) or closed (on presumed depolarizing bipolar cells) by the probable photoreceptor transmitter, glutamate, will contribute significant noise to the membrane voltage in the dark. In hyperpolarizing bipolar cells the noise will have a standard deviation of 300–400 μV. In depolarizing bipolar cells, the noise will be in the range 340–600 μV. Voltage noise will also be generated in these cells by any channels opened by GABA or glycine in the dark, but we are unable to estimate the magnitude of this noise because the sizes of the currents carried by these channels in the intact retina are unknown. By adding the variances of the voltage noise produced by the non-synaptic channels and the glutamate-gated channels, we can calculate that the standard deviation of the noise due to both sources will be in the range 310–490 μV for hyperpolarizing bipolar cells and 350–670 μV for depolarizing cells. Even taking the lower limits for each cell type, these levels of noise would hinder

the detection of signals of less than 600–700 μV amplitude (twice the standard deviation).

Channel noise can therefore, in principle, limit the detection of weak signals. Just how significant a limit it represents depends on whether *all* of the noise generated by channels hinders signal detection, or whether noise outside the frequency range of the light-evoked signal is irrelevant because it is filtered out at later stages of the visual system. In addition, whether channel noise is the *principal* limit on signal detection depends on the magnitude of two other sources of noise in the intact retina: noise generated in photoreceptors (Simon, Lamb & Hodgkin, 1975; Schwartz, 1977) and transmitted synaptically, and noise arising from the quantal nature of transmitter release from cells presynaptic to the bipolar cells. These sources have been studied in turtle and dogfish, but not axolotl. Ashmore & Copenhagen (1983) estimated that about 75% of the light-suppressed voltage noise variance in turtle hyperpolarizing bipolar cells originated in presynaptic cones. Similarly, for dogfish depolarizing bipolar cells, Ashmore & Falk (1982) calculated that about 60% of the light-suppressed noise was transmitted from presynaptic rods. In both cases the remaining light-sensitive noise was assumed to be introduced during synaptic transmission, as fluctuations in quantal release and post-synaptic channel noise. In turtle hyperpolarizing bipolar cells this 'synaptic' voltage noise had a standard deviation of about 600 μV, i.e. slightly larger than the 300–400 μV of noise we predict would be generated by the glutamate-gated channels (assuming these channels have the same properties in both species). In dogfish depolarizing cells, the 'synaptic' noise had a standard deviation of about 180 μV, while we predict the glutamate-gated channels would generate 150–300 μV of noise (this is smaller than the estimate for axolotl given earlier because of the lower resistance of dogfish cells). Comparison of the exact magnitudes of presynaptic noise and noise introduced during synaptic transmission must await detailed studies on a single species.

We thank David Colquhoun and Armand Cachelin for computer facilities, Tim Biscoe, Lillian Patterson and Michael Duchen for advice on ionophoretic experiments, Lindsey Alldritt for secretarial assistance and Jerry Lockett for photographic services. This work was supported by the M.R.C., the Wellcome Trust, the Nuffield Foundation, Fight for Sight (U.K.), NATO (Collaborative Research Grant RG.85/0471), the Central Research Fund of London University, N.I.H. (EY 04112) to M.W., the British Council (M.T.-L.) and the Royal Society (D.A.). Some of this work was submitted by M.T.-L. as part of a PhD Thesis in the University of London.

REFERENCES

ANDERSON, C. R., CULL-CANDY, S. G. & MILEDI, R. (1978). Glutamate current noise: post-synaptic channel kinetics investigated under voltage clamp. *Journal of Physiology* **282**, 219–242.

ANDERSON, C. R. & STEVENS, C. F. (1973). Voltage clamp analysis of acetylcholine produced end-plate current fluctuations at frog neuromuscular junction. *Journal of Physiology* **235**, 655–691.

ASHMORE, J. F. & COPENHAGEN, D. R. (1980). Different postsynaptic events in two types of retinal bipolar cell. *Nature* **288**, 84–86.

ASHMORE, J. F. & COPENHAGEN, D. R. (1983). An analysis of transmission from cones to hyperpolarizing bipolar cells in the retina of the turtle. *Journal of Physiology* **340**, 569–597.

ASHMORE, J. F. & FALK, G. (1980). Responses of rod bipolar cells in the dark-adapted retina of the dogfish, *Scyliorhinus canicula*. *Journal of Physiology* **300**, 115–150.

ASHMORE, J. F. & FALK, G. (1982). An analysis of voltage noise in rod bipolar cells of the dogfish retina. *Journal of Physiology* **332**, 273–297.

ATTWELL, D. (1986). Ion channels and signal processing in the outer retina. The Sharpey-Schafer lecture. *Quarterly Journal of Experimental Physiology* **71**, 497–536.

ATTWELL, D., WERBLIN, F. S. & WILSON, M. (1982). The properties of single cones isolated from the tiger salamander retina. *Journal of Physiology* **328**, 259–283.

ATTWELL, D., WERBLIN, F. S., WILSON, M. & WU, S. M. (1983). A sign-reversing pathway from rods to double and single cones in the retina of the tiger salamander. *Journal of Physiology* **336**, 313–333.

ATTWELL, D. & WILSON, M. (1980). Behaviour of the rod network in the tiger salamander retina mediated by membrane properties of individual rods. *Journal of Physiology* **309**, 287–315.

BADER, C. R., MACLEISH, P. R. & SCHWARTZ, E. A. (1979). A voltage-clamp study of the light response in solitary rods of the turtle. *Journal of Physiology* **296**, 1–26.

BAYLOR, D. A. & FETTIPLACE, R. (1977). Kinetics of synaptic transfer from receptors to ganglion cells in turtle retina. *Journal of Physiology* **271**, 425–448.

BAYLOR, D. A., FUORTES, M. G. F. & O'BRYAN, P. M. (1971). Receptive fields of cones in the retina of the turtle. *Journal of Physiology* **214**, 265–294.

BENDAT, J. S. & PIERSOL, A. G. (1971). *Random Data.* New York: Wiley-Interscience.

BORGES, S. & WILSON, M. (1984). Measurement of bipolar cell receptive field centre size for tiger salamander retina. *Society for Neuroscience Abstracts* **10**, 324.

CAHALAN, M. D., CHANDY, K. G., DECOURSEY, T. E. & GUPTA, S. (1985). A voltage-gated K^+ channel in human T lymphocytes. *Journal of Physiology* **358**, 197–237.

CAJAL, S. R. (1983). La rétine des vertèbres. *La Cellule* **9**, 17–257.

CERVETTO, L. & MACNICHOL JR, E. F. (1972). Inactivation of horizontal cells in turtle retina by glutamate and aspartate. *Science* **178**, 767–768.

CHIU, C-A. & LAM, D. M. K. (1980). The uptake and release of [^{3}H]-glycine in the goldfish retina. *Journal of Physiology* **308**, 185–195.

COLQUHOUN, D., DREHER, F. & SHERIDAN, R. E. (1979). The actions of tubocurarine at the frog neuromuscular junction. *Journal of Physiology* **293**, 247–284.

COLQUHOUN, D. & HAWKES, A. G. (1977). Relaxation and fluctuations of membrane currents that flow through drug-operated channels. *Proceedings of the Royal Society* B **199**, 231–262.

CONNOR, J. A. & STEVENS, C. F. (1971*a*). Inward and delayed outward membrane currents in isolated neural somata under voltage clamp. *Journal of Physiology* **213**, 1–19.

CONNOR, J. A. & STEVENS, C. F. (1971*b*). Voltage-clamp studies of a transient outward current in gastropod neural somata. *Journal of Physiology* **213**, 21–30.

CULL-CANDY, S. G. & OGDEN, D. C. (1985). Ion channels activated by L-glutamate and GABA in cultured cerebellar neurones of the rat. *Proceedings of the Royal Society* B **224**, 367–373.

DETWILER, P. B., HODGKIN, A. L. & MCNAUGHTON, P. A. (1978). A surprising property of electrical spread in the network of rods in the turtle's retina. *Nature* **274**, 562–565.

DIONNE, V. E. (1976). Characterization of drug iontophoresis with a fast microassay technique. *Biophysical Journal* **16**, 705–717.

FALK, G. & FATT, P. (1974). Limitations to single photon sensitivity in vision. In *Lecture Notes in Mathematics*, vol. 4, *Physics and Mathematics of the Nervous System*, ed. CONRAD, M., GÜTTINGER, W. & DAL CIN, M., pp. 171–204. Berlin: Springer.

FENWICK, E. M., MARTY, A. & NEHER, E. (1982). A patch-clamp study of bovine chromaffin cells and of their sensitivity to acetylcholine. *Journal of Physiology* **331**, 577–597.

FUKUSHIMA, Y., HAGIWARA, S. & HENKART, M. (1984). Potassium current in clonal cytotoxic T lymphocytes. *Journal of Physiology* **351**, 645–656.

HAMILL, O. P., BORMANN, J. & SAKMANN, B. (1983). Activation of multiple state chloride channels in spinal neurones by glycine and GABA. *Nature* **305**, 805–808.

HAMILL, O. P., MARTY, A., NEHER, E., SAKMANN, B. & SIGWORTH, F. J. (1981). Improved patch-clamp methods for recording from cells and cell-free membrane patches. *Pflügers Archiv* **391**, 85–100.

HARE, W. A., CAPOVILLA, M. & OWEN, W. G. (1984). Functional properties of histologically identified bipolar cells in the salamander retina. *Investigative Ophthalmology*, suppl. **25**, 237.

HOLLYFIELD, J. G., RAYBORN, M. E., SARTHY, P. V. & LAM, D. M. K. (1979). The emergence, localization and maturation of neurotransmitter systems during development of the retina in *Xenopus laevis*: I. γ-aminobutyric acid. *Journal of Comparative Neurology* **188**, 587–598.

ISHIDA, A. T., KANEKO, A. & TACHIBANA, M. (1984). Responses of solitary retinal horizontal cells from *Carassius auratus* to L-glutamate and related amino acids. *Journal of Physiology* **348**, 255–270.

ISHIDA, A. T. & NEYTON, J. (1985). Quisqualate and L-glutamate inhibit retinal horizontal cell responses to kainate. *Proceedings of the National Academy of Sciences of the U.S.A.* **82**, 1837–1841.

KANEKO, A. (1971). Physiological studies of single retinal cells and their morphological identification. *Vision Research* **3**, suppl., 17–26.

KANEKO, A. & TACHIBANA, M. (1985). A voltage-clamp analysis of membrane currents in solitary bipolar cells dissociated from *Carassius auratus*. *Journal of Physiology* **358**, 131–152.

LANDOLT, E. (1871). Beitrage zur Anatomie der Retina von Frosch, Salamander und Triton. *Archiv fur Mikroskopische Anatomie und Entwicklungsmechanik* **7**, 81–100.

LASANSKY, A. (1973). Organisation of the outer synaptic layer in the retina of the larval tiger salamander. *Proceedings of the Royal Society* B **265**, 471–489.

LASANSKY, A. (1978). Contacts between receptors and electrophysiologically identified neurones in the retina of the larval tiger salamander. *Journal of Physiology* **285**, 531–542.

LASATER, E. M., DOWLING, J. E. & RIPPS, H. (1984). Pharmacological properties of isolated horizontal and bipolar cells from the skate retina. *Journal of Neuroscience* **4**, 1966–1975.

MARC, R. E., STELL, W. K., BOK, D. & LAM, D. M. K. (1978). GABA-ergic pathways in the goldfish retina. *Journal of Comparative Neurology* **182**, 221–246.

MARR, D. & HILDRETH, E. (1980). Theory of edge detection. *Proceedings of the Royal Society* B **207**, 187–217.

MARR, D. & ULLMAN, S. (1981). Directional sensitivity and its use in early visual processing. *Proceedings of the Royal Society* B **211**, 151–180.

MATTHEWS-BELLINGER, J. & SALPETER, M. (1978). Distribution of acetylcholine receptors at frog neuromuscular junctions with a discussion of some physiological implications. *Journal of Physiology* **279**, 197–213.

MILLER, A. M. & SCHWARTZ, E. A. (1983). Evidence for the identification of synaptic transmitters released by photoreceptors of the toad retina. *Journal of Physiology* **334**, 325–350.

MILLER, R. F. & DACHEUX, R. F. (1976). Synaptic organization and ionic basis of on and off channels in mudpuppy retina. III. A model of ganglion cell receptive field organization based on chloride-free experiments. *Journal of General Physiology* **67**, 679–690.

MILLER, R. F. & DACHEUX, R. F. (1983). Intracellular chloride in retinal neurones: measurement and meaning. *Vision Research* **23**, 399–411.

MILLER, R. F., FRUMKES, T. E., SLAUGHTER, M. & DACHEUX, R. F. (1981). Physiological and pharmacological basis of GABA and glycine action on neurons of mudpuppy retina. I. Photoreceptors, horizontal cells, bipolar cells and ganglion cells. *Journal of Neurophysiology* **45**, 743–763.

MURAKAMI, M., OHTSU, K. & OHTSUKA, T. (1972). Effects of chemicals on receptors and horizontal cells in the retina. *Journal of Physiology* **227**, 899–913.

NOWAK, L., BREGESTOVSKI, P., ASCHER, P., HERBERT, A. & PROCHIANTZ, A. (1984). Magnesium gates glutamate-activated channels in mouse central neurones. *Nature* **307**, 462–465.

RAYBORN, M. E., SARTHY, P. V., LAM, D. M. K. & HOLLYFIELD, J. G. (1981). The emergence, localization and maturation of neurotransmitter systems during development of the retina in *Xenopus laevis*: II. Glycine. *Journal of Comparative Neurology* **195**, 585–593.

SAITO, T., KONDO, H. & TOYODA, J. (1978). Rod and cone signals in the on-center bipolar: their different ionic mechanisms. *Vision Research* **18**, 591–595.

SCHANTZ, M. & NAKA, K. I. (1976). The bipolar cell. *Biophysical Journal* **16**, 1517–1518.

SCHWARTZ, E. A. (1974). Responses of bipolar cells in the retina of the turtle. *Journal of Physiology* **236**, 211–224.

SCHWARTZ, E. A. (1977). Voltage noise observed in rods of the turtle retina. *Journal of Physiology* **272**, 217–246.

SCHWARTZ, E. A. (1982). Calcium-independent release of GABA from isolated cells of the toad retina. *Journal of Physiology* **323**, 211–228.

SHIELLS, R. A., FALK, G. & NAGHSHINEH (1981). Action of glutamate and aspartate analogues on rod horizontal and bipolar cells. *Nature* **294**, 592–594.

SIMMONDS, M. A. (1983). Multiple GABA receptors and associated regulatory sites. *Trends in Neuroscience* **6**, 279–281.

SIMON, E. J., LAMB, T. & HODGKIN, A. L. (1975). Spontaneous voltage fluctuations in retinal cones and bipolar cells. *Nature* **256**, 661–662.

SLAUGHTER, M. M. & MILLER, R. F. (1981). 2-Amino-4-phosphonobutyric acid: a new pharmacological tool for retina research. *Science* **211**, 182–185.

SLAUGHTER, M. M. & MILLER, R. F. (1983*a*). The role of excitatory amino acid transmitters in the mudpuppy retina: an analysis with kainic acid and *N*-methylaspartate. *Journal of Neuroscience* **3**, 1701–1711.

SLAUGHTER, M. M. & MILLER, R. F. (1983*b*). An excitatory amino acid antagonist blocks cone input to sign-conserving second-order retinal neurones. *Science* **219**, 1230–1232.

SLAUGHTER, M. M. & MILLER, R. F. (1985). Characterization of an extended glutamate receptor of the on bipolar neuron in the vertebrate retina. *Journal of Neuroscience* **5**, 224–233.

SMITH, R. M. & MARTELL, A. E. (1976). *Critical Stability Constants*, vol. 4, *Inorganic Complexes*. New York and London: Plenum Press.

SRINIVASAN, M. V., LAUGHLIN, S. B. & DUBS, A. (1982). Predictive coding: a fresh view of inhibition in the retina. *Proceedings of the Royal Society* B **216**, 427–459.

TACHIBANA, M. (1985). Permeability changes induced by L-glutamate in solitary retinal horizontal cells isolated from *Carassius auratus*. *Journal of Physiology* **358**, 153–167.

TACHIBANA, M. & KANEKO, A. (1984). γ-Aminobutyric acid acts at axon terminals of turtle photoreceptors: difference in sensitivity among cell types. *Proceedings of the National Academy of Sciences of the U.S.A.* **81**, 7961–7964.

TOYODA, J. (1973). Membrane resistance changes underlying the bipolar response in carp retina. *Vision Research* **13**, 283–294.

WERBLIN, F. S. (1978). Transmission along and between rods in the tiger salamander retina. *Journal of Physiology* **280**, 449–470.

WERBLIN, F. S. & DOWLING, J. E. (1969). Organization of the retina of the mudpuppy, *Necturus maculosus*. II. Intracellular recording. *Journal of Neurophysiology* **32**, 339–355.

WONG-RILEY, M. T. T. (1974). Synaptic organization of the inner plexiform layer in the retina of the tiger salamander. *Journal of Neurocytology* **3**, 1–33.

WU, S. M. (1986). Effects of γ-aminobutyric acid on cones and bipolar cells of the tiger salamander retina. *Brain Research* **365**, 70–77.